Journal of Medicinal Chemistry

pubs.acs.org/jmc

Article

From Celecoxib to a Novel Class of Phosphodiesterase 5 Inhibitors: Trisubstituted Pyrazolines as Novel Phosphodiesterase 5 Inhibitors with Extremely High Potency and Phosphodiesterase Isozyme Selectivity

Mohammad Abdel-Halim,* Sara Sigler, Nora A. S. Racheed, Amr Hefnawy, Reem K. Fathalla, Mennatallah A. Hammam, Ahmed Maher, Yulia Maxuitenko, Adam B. Keeton, Rolf W. Hartmann, Matthias Engel, Gary A. Piazza, and Ashraf H. Abadi*

Cite This: *J. Med. Chem.* 2021, 64, 4462−4477

Read Online

ACCESS | Metrics & More | Article Recommendations | Supporting Information

ABSTRACT: A ligand-based approach involving systematic modifications of a trisubstituted pyrazoline scaffold derived from the COX2 inhibitor, celecoxib, was used to develop novel PDE5 inhibitors. Novel pyrazolines were identified with potent PDE5 inhibitory activity lacking COX2 inhibitory activity. Compound **d12** was the most potent with an IC_{50} of 1 nM, which was three times more potent than sildenafil and more selective with a selectivity index of >10,000-fold against all other PDE isozymes. Sildenafil inhibited the full-length and catalytic fragment of PDE5, while compound **d12** only inhibited the full-length enzyme, suggesting a mechanism of enzyme inhibition distinct from sildenafil. The PDE5 inhibitory activity of compound **d12** was confirmed in cells using a cGMP biosensor assay. Oral administration of compound **d12** achieved plasma levels >1000-fold higher than IC_{50} values and showed no discernable toxicity after repeated dosing. These results reveal a novel strategy to inhibit PDE5 with unprecedented potency and isozyme selectivity.

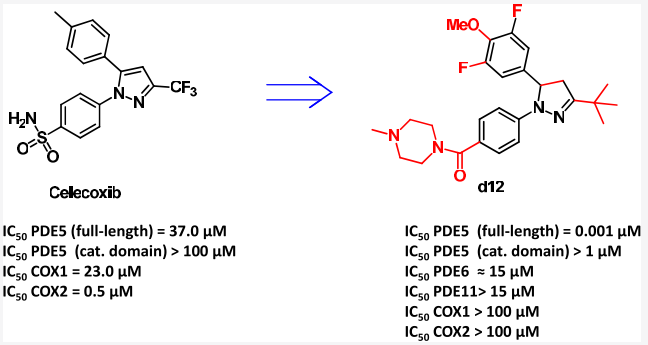

INTRODUCTION

Celecoxib is a non-steroidal anti-inflammatory drug (NSAID) approved for the treatment of pain and swelling associated with rheumatoid arthritis or osteoarthritis. Celecoxib (4-[5-(4-methylphenyl)-3-(trifluoromethyl)-1*H*-pyrazol-1-yl]-benzenesulfonamide),[1] unlike other NSAIDs that suppress prostaglandin synthesis by non-selective inhibition of cyclo-oxygenases types 1 and 2 (COX1 and COX2), belongs to a distinct subclass of NSAIDs referred to as coxibs that selectively inhibit the inducible COX2 isozyme. By sparing COX1 and physiological levels of prostaglandins, coxibs were developed to reduce the risk of gastric ulceration and other toxicities associated with the inhibition of constitutively expressed COX1.[2] After FDA approval of several coxibs, prolonged use was unexpectedly found to have cardiovascular toxicities, including myocardial infarction and stroke.[3,4] These toxicities are linked to imbalance between prostacyclin and thromboxane levels, in which the biosynthesis of the former is suppressed by selective COX2 inhibitors.[5−7] Unlike other COX2 inhibitors, such as rofecoxib that was withdrawn from the market because of risks associated with cardiovascular toxicity, celecoxib is still marketed and is considered to be less cardiotoxic. The reduced toxicity of celecoxib may be partly attributed to an off-target mechanism involving the inhibition of phosphodiesterase 5 (PDE5), which leads to vasodilatation that may offset the vasoconstriction resulting from inhibition of prostacyclin biosynthesis.[8−11]

PDE5 is a cGMP-specific PDE that plays an important role in the regulation of cGMP levels in multiple cell types.[12−14] Like all PDEs, PDE5 is a dimeric protein, each monomer consisting of a C-terminal catalytic domain and N-terminal regulatory domain.[14] The regulatory domain of PDE5 contains tandem GAF domains (GAF-A and GAF-B) and a site for phosphorylation by cyclic nucleotide-dependent protein kinases. PDE5 is allosterically regulated by binding of cGMP to GAF-A domain, leading to an increase in its enzymatic activity.[15,16]

Received: June 30, 2020
Published: April 1, 2021

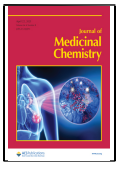

PDE5 is highly abundant in smooth muscle cells and plays an important role in regulating contractility.[16] PDE5 became an important therapeutic target for the treatment of erectile dysfunction and pulmonary arterial hypertension, which led to the development of potent PDE5 inhibitors, such as sildenafil, vardenafil, and tadalafil.[17,18]

More recently, several potent PDE5 inhibitors were reported; however, they show significant cross-reactivity with PDE6 and PDE11, similar to currently approved PDE5 inhibitors.[19−22] Fiorito et al. reported a highly potent tetrahydrobenzo[*b*][1,6]naphthyridine derivative with about 500-fold selectivity vs PDE6; however, no selectivity data were provided regarding the other PDE isoforms.[23]

All the classical PDE5 inhibitors like sildenafil, vardenafil, and tadalafil are known to act through binding within the catalytic domain of PDE5, competing with cGMP.[24−26] However, it was reported that the N-terminal 46 amino acids in GAF-B domain (Glu420 through Gly466) are required for high potency of vardenafil but not for sildenafil, despite having a similar mode of binding, as shown in cocrystal structures.[27]

Here, we show that the previously reported off-target activity of celecoxib on PDE5 occurs by a unique mechanism of inhibition that requires the presence of the regulatory domain. As described below, we employed a ligand-based approach to uncouple PDE5 and COX2 inhibitory activities using a pyrazoline scaffold derived from celecoxib. A novel series of pyrazolines were found with high potency and selectivity to inhibit PDE5 while lacking COX2 inhibitory activity, providing distinct advantages over currently available PDE5 inhibitors.

RESULTS AND DISCUSSION

Synthetic Strategy and Approach. Our rationale to develop novel PDE5 inhibitors was inspired from previous studies suggesting that celecoxib inhibits PDE5 and from our earlier synthetic efforts, which revealed that certain pyrazoline derivatives yielded PDE5 inhibitors with improved potency. To this end, we characterized the PDE5 inhibitory activity of celecoxib using the PDE5 catalytic domain as well as the full-length enzyme and compared its inhibitory activity with sildenafil. As anticipated, sildenafil inhibited both the catalytic domain and the full-length enzyme with IC_{50} values of 4.9 and 3 nM, respectively.[27] Surprisingly, celecoxib was found to only inhibit the full-length enzyme, with an IC_{50} of 37 μM, whereas the activity of the catalytic domain was not affected at concentrations up to 100 μM. Figure 1 shows the dose−response curves for sildenafil and celecoxib against both the PDE5 catalytic domain and the full-length PDE5. These results suggested that celecoxib inhibits PDE5 by a mechanism that is different from conventional PDE5 inhibitors, which compete with cGMP for binding to the catalytic domain. Instead, celecoxib appeared to exert a mode of action that was strictly dependent on the regulatory domain. Thus, relying on binding to a less conserved regulatory site, celecoxib was identified as a promising lead compound to develop a new class of inhibitors with better selectivity profile over classical substrate-competitive inhibitors.[28] Applying a ligand-based approach starting from celecoxib, systematic structural modifications were undertaken to enhance potency and selectivity to inhibit PDE5.

Our initial synthetic efforts aimed at enhancing the PDE5 inhibitory activity of celecoxib while abolishing its COX2 inhibitory action by modulating essential features required for COX2 inhibition.[1] This was successfully done by replacement

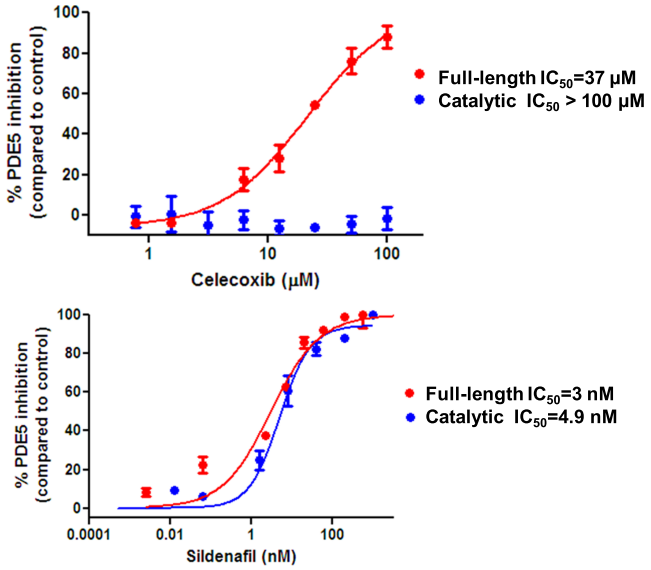

Figure 1. Inhibition of PDE5 full length vs the catalytic domain by celecoxib and sildenafil.

of the sulfonamide group at the 1-phenyl with a carboxylic acid functional group. The second modification was the replacement of trifluoromethyl group with *t*-butyl at position 3 of the pyrazole. Finally, partial saturation of the pyrazole to the non-coplanar Δ^2-pyrazoline was found to improve PDE5 inhibitory potency. These modifications led to compound **A** (Figure 2) with an IC_{50} of 8.4 μM against PDE5, giving more than 4-fold improved potency compared to celecoxib (IC_{50} = 37 μM). The subsequent optimization of compound **A** involved the replacement of the 4-tolyl moiety by several mono-substituted aryls (details are recently published);[29] this led to compound **B** that has a 4-methoxyphenyl group replacing the 4-tolyl (Figure 2). Compound **B** showed a further 4-fold increase in potency against PDE5 (IC_{50} = 2 μM). In this work, compound **B** was selected as a template for optimization and to explore SAR, as discussed in the following sections (Figure 2). The details of modifications of celecoxib to compounds **A** and **B** have been recently published.[29]

Chemical Synthesis. The synthesis of the pyrazoline derivatives was performed in two steps. In the first step, the required enones were furnished through a Claisen−Schmidt condensation between aromatic aldehydes and pinacolone or acetophenone analogues. In the second step, the respective enones were reacted with 4-hydrazinobenzoic acid hydrochloride to yield the desired pyrazolines using the previously reported regioselective synthesis of 1,3,5-triarylpyrazolines (Schemes 1 and 2).[30] Following a rigidification strategy, bridging atom(s), particularly, $-CH_2-$ (**a48**), $-CH_2-CH_2-$ (**a49**), or $-O-CH_2-$ (**a50**), were introduced between the phenyl at position 3 and C-4 of the original 1,3,5-trisubstituted pyrazoline system (Scheme 2).

The chemical optimization included three rounds of synthesis, each of which was followed by biological evaluation, in which the first round involved simple variations of compound **B** with substitutions at positions 3 and 5, as shown in Figure 2. A second round of optimization involved extending the substitution at position 1 from a carboxylic acid with various amide derivatives. Amides were synthesized by the reaction of the benzoic acid derivatives with the suitable amine precursor using EDCI·HCl as a coupling agent in CH_2Cl_2

https://doi.org/10.1021/acs.jmedchem.0c01120
J. Med. Chem. 2021, 64, 4462−4477

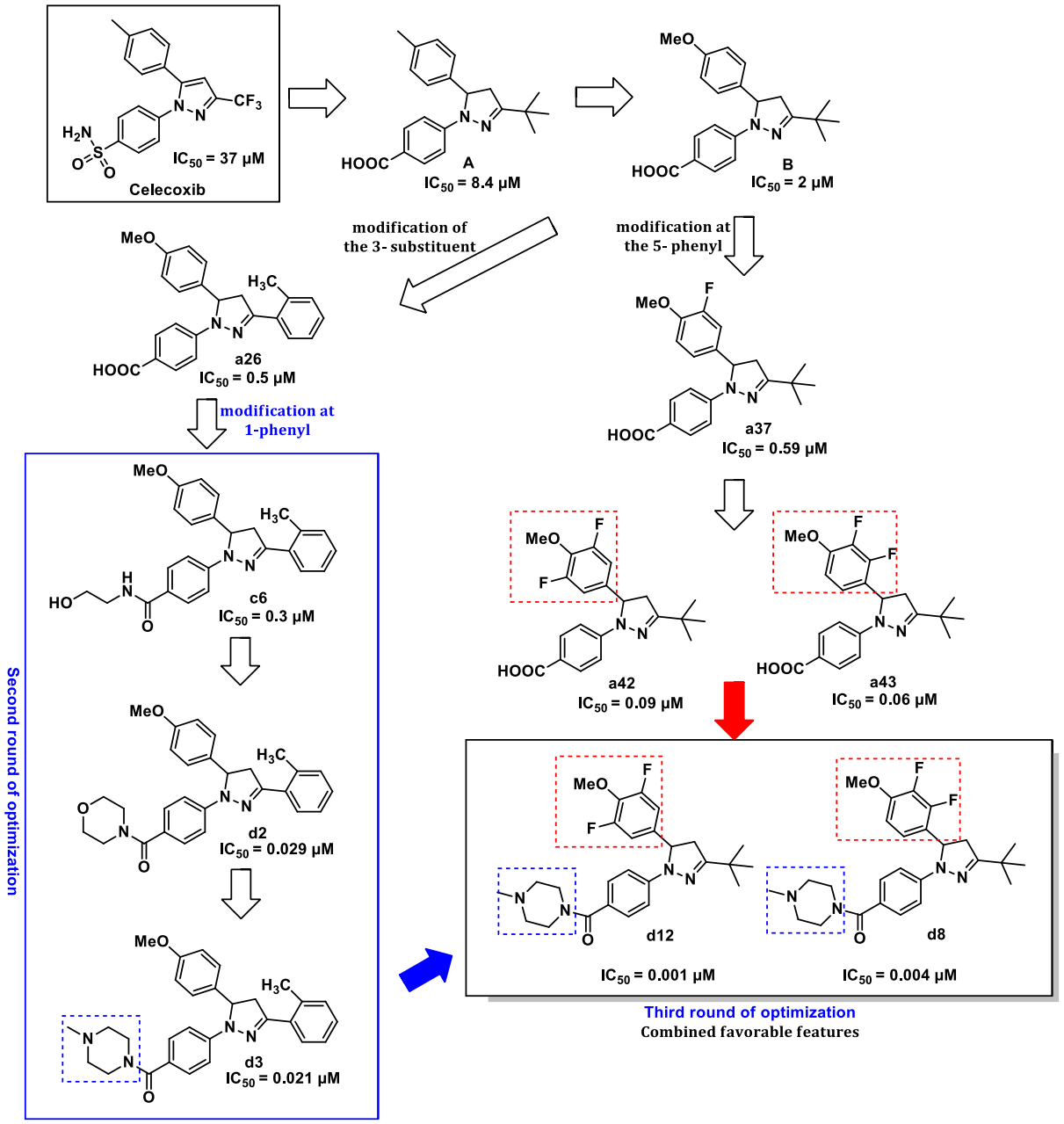

Figure 2. Optimization of the PDE5 inhibitory activity starting from celecoxib.

(Scheme 3). A third round included combining the favorable structural features obtained from the first two rounds (Figure 2). To confirm the importance of the non-coplanar pyrazoline system for the PDE5 activity, compounds **a4** and **d9** were oxidized to the corresponding pyrazole analogues using DDQ in refluxing benzene (Schemes 1 and 3).

Biological Activity. All the benzoic acid derivatives and the amides were evaluated for their ability to inhibit full-length recombinant PDE5. Each compound was evaluated in two steps. For the first screening step, the percentage of PDE5 inhibition was determined at a concentration of 10 μM. Compounds showing greater than 50% inhibition were re-tested with an extended concentration range to determine PDE5 inhibitory potency by calculation of IC_{50} values. The results for PDE5 inhibition are shown in Tables 1−3. Additionally, some compounds showing potent PDE5 inhibition were screened against COX1 and COX2 at 50 μM. All compounds tested were inactive against COX1 and COX2 at the screening dose (Table S1, Supporting Information).

Structure−Activity Relationships (SAR) for PDE5 inhibitory activity. First Round of Optimization. To optimize the PDE5 inhibitory activity of compound **B**, we started the modifications at two major sites: the first at position 3 of the pyrazoline and the second at the 5-phenyl.

Modifications at Position 3 of the Pyrazoline. The modifications at position 3 were started by replacing the *tert*-butyl group in compound **B** by alicyclic groups like cyclopropyl, 1-methylcyclopropyl, and cyclohexyl (compounds **a1**−**a3**, respectively), which led to a loss of activity. This finding emphasizes the important role of a bulky and highly branched alkyl to maintain activity, indicating that the higher branching of the *tert*-butyl group is more favored by the binding pocket. On the other hand, the replacement of the *tert*-

https://doi.org/10.1021/acs.jmedchem.0c01120
J. Med. Chem. 2021, 64, 4462−4477

Scheme 1

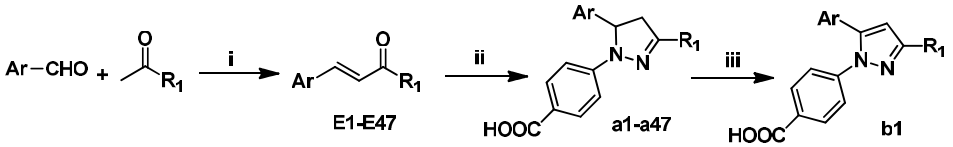

Reagents and conditions: (i) 10%KOH, MeOH, ice cooling then room temperature, overnight (ii) 1.5 equiv 4-hydrazinobenzoic acid hydrochloride, DMF, 85 °C, 5h. (iii) 1.5 equiv DDQ, benzene, reflux, 5h.

Cpd #	E	Ar	R_1
A	A	4-tolyl	*t*-Bu
B	B	4-methoxyphenyl	*t*-Bu
a1	1	4-methoxyphenyl	cyclopropyl
a2	2	4-methoxyphenyl	1-methylcyclopropyl
a3	3	4-methoxyphenyl	cyclohexyl
a4	4	4-methoxyphenyl	phenyl
a5	5	4-methoxyphenyl	pyrrol-2-yl
a6	6	4-methoxyphenyl	pyridin-2-yl
a7	7	4-methoxyphenyl	thiophen-2-yl
a8	8	4-methoxyphenyl	furan-2-yl
a9	9	4-methoxyphenyl	napthalen-1-yl
a10	10	4-methoxyphenyl	4-phenoxyphenyl
a11	11	4-methoxyphenyl	[1,1'-biphenyl]-4-yl
a12	12	4-methoxyphenyl	benzo[d][1,3]dioxol-5-yl
a13	13	4-methoxyphenyl	2-methoxyphenyl
a14	14	4-methoxyphenyl	3-methoxyphenyl
a115	15	4-methoxyphenyl	4-methoxyphenyl
a16	16	4-methoxyphenyl	3,4-dimethoxyphenyl
a17	17	4-methoxyphenyl	2-fluorophenyl
a18	18	4-methoxyphenyl	3-fluorophenyl
a19	19	4-methoxyphenyl	4-fluorophenyl
a20	20	4-methoxyphenyl	2-chlorophenyl
a21	21	4-methoxyphenyl	3-chlorophenyl
a22	22	4-methoxyphenyl	4-chlorophenyl
a23	23	4-methoxyphenyl	2,4-dichlorophenyl
a24	24	4-methoxyphenyl	2-bromophenyl
a25	25	4-methoxyphenyl	4-bromophenyl
a26	26	4-methoxyphenyl	*o*-tolyl
a27	27	4-methoxyphenyl	*m*-tolyl
a28	28	4-methoxyphenyl	*p*-tolyl
a29	29	4-methoxyphenyl	2-hydroxyphenyl
a30	30	4-methoxyphenyl	3-hydroxyphenyl
a31	31	4-methoxyphenyl	4-hydroxyphenyl
a32	32	4-methoxyphenyl	2-ethoxyphenyl
a33	33	4-methoxyphenyl	4-ethoxyphenyl
a34	34	4-methoxyphenyl	2-nitrophenyl
a35	35	3-Fluoro-4-methoxyphenyl	phenyl
a36	36	3-Fluoro-4-methoxyphenyl	*o*-tolyl
a37	37	3-fluoro-4-methoxyphenyl	*t*-Bu
a38	38	4-trifluoromethylphenyl	*t*-Bu
a39	39	4-trifluoromethoxyphenyl	*t*-Bu
a40	40	4-fluoro-3-methoxyphenyl	*t*-Bu
a41	41	3-chloro-4-methoxyphenyl	*t*-Bu
a42	42	3,5-difluoro-4-methoxyphenyl	*t*-Bu
a43	43	2,3-difluoro-4-methoxyphenyl	*t*-Bu
a44	44	2,5-difluoro-4-methoxyphenyl	*t*-Bu
a45	45	3,5-difluorophenyl	*t*-Bu
a46	46	3-fluoro-4-methylphenyl	*t*-Bu
a47	47	3,5-difluoro-4-ethoxyphenyl	*t*-Bu
b1	-	4-methoxyphenyl	phenyl

Scheme 2

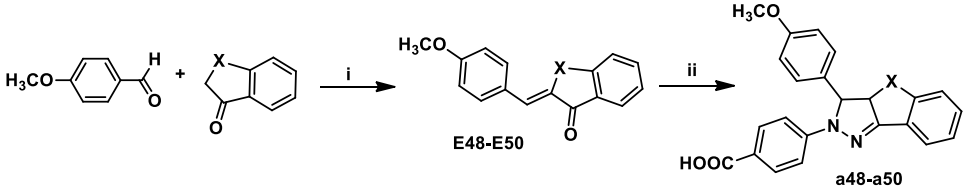

Reagents and conditions: (i) 10% KOH, MeOH, ice cooling then room temperature, overnight (ii) 1.5 equiv 4-hydrazinobenzoic acid hydrochloride, DMF, 85 °C, 5h.

Cpd #	X	E
a48	-CH_2-	48
a49	-CH_2CH_2-	49
a50	-O-CH_2- (O next to Ph)	50

butyl in **B** by a phenyl ring slightly improved the potency, suggesting that additional CH−π interactions were formed (compound **a4**; IC_{50} = 1.2 μM). This is especially evident by comparing the cyclohexyl analogue, **a3**, to **a4**. However, when other derivatives with aromatic heterocyclic substitutions such as pyrrole, pyridine, thiophene, and furan were synthesized, the activity was completely abolished (compounds **a5**−**a8**, respectively). Additionally, the use of bulkier aromatic systems

https://doi.org/10.1021/acs.jmedchem.0c01120
J. Med. Chem. 2021, 64, 4462−4477

Scheme 3

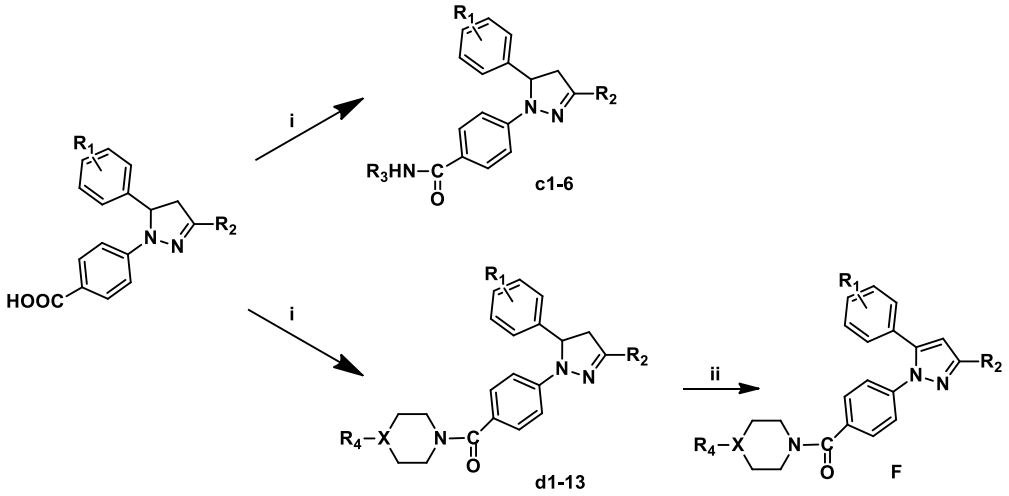

Reagents and conditions: Amine derivative, EDCI, CH_2Cl_2, room temperature, overnight. (ii) 1.5 equiv DDQ, benzene, reflux, 5h.

Cpd #	R_1	R_2	R_3	R4	X
c1	4-methoxy	phenyl	n-butyl	-	-
c2	4-methoxy	phenyl	ethyl	-	-
c3	4-methoxy	*t*-Bu	n-butyl	-	-
c4	3-fluoro-4-methoxy	*t*-Bu	n-butyl	-	-
c5	4-methoxy	*o*-tolyl	n-butyl	-	-
c6	4-methoxy	*o*-tolyl	2-hydroxyethyl	-	-
d1	4-methoxy	phenyl	-	methyl	N
d2	4-methoxy	*o*-tolyl	-	-	O
d3	4-methoxy	*o*-tolyl	-	methyl	N
d4	3-fluoro-4-methoxy	*o*-tolyl	-	methyl	N
d5	3-fluoro-4-methoxy	*t*-Bu	-	methyl	N
d6	4-fluoro-3-methoxy	*t*-Bu	-	methyl	N
d7	3-chloro-4-methoxy	*t*-Bu	-	methyl	N
d8	2,3-difluoro-4-methoxy	*t*-Bu	-	methyl	N
d9	3,5-difluoro-4-ethoxy	t-Bu	-	methyl	N
d10	3-fluoro-4-methyl	*t*-Bu	-	methyl	N
d11	4-methoxy	*t*-Bu	-	methyl	N
d12	3,5-difluoro-4-methoxy	*t*-Bu	-	methyl	N
d13	2,5-difluoro-4-methoxy	*t*-Bu	-	methyl	N
F	3,5-difluoro-4-ethoxy	*t*-Bu	-	methyl	N

such as 1-napthyl, 4-biphenyl, and 4-phenoxyphenyl at position 3 of the pyrazoline (compounds **a9**−**a11**, respectively) led to loss of activity, which might be due to the higher steric demand of these aromatic systems that are not tolerated within the binding pocket. Even the use of more polar methylenedioxyphenyl (compound **a12**) did not recover the potency to inhibit PDE5. Interestingly, compound **a16** with the 3,4-dimethoxyphenyl group that is the open-chain analogue of compound **a12** showed moderate PDE5 inhibitory activity, indicating a possible steric clash between the methylene bridge in **a12** and the PDE5 binding pocket.

Next, we investigated the effect of adding different types of substituents at the 3-phenyl ring of compound **a4**. Initially, a mono-halogen substitution with chlorine, bromine, and fluorine at different positions on the phenyl ring in compound **a4** was synthesized to give compounds **a17**−**a22** and **a24** and **a25**. This resulted in loss of the PDE5 inhibitory activity (IC_{50} > 10 μM) apart from compound **a19** having a *para*-fluoro substitution. The loss of PDE5 inhibitory activity might be either due to the non-tolerated lipophilic and steric nature of the substituents or because of their electron-withdrawing property, which decreases the π-electron density on the phenyl ring and might be unfavorable here. Consequently, compound **a23** with a 2,4-dichloro substitution was found to be inactive, too. On the other hand, a hydrophilic electron-donating substituent like a hydroxyl group showed the best activity at the *ortho* position in compound **a29** with more than a 3-fold improvement in potency compared to the unsubstituted phenyl in compound **a4**, while at the *para* position, the hydroxyl group was tolerated with a 2-fold decrease in PDE5 inhibitory potency (compound **a31** compared to **a4**). Moving the hydroxyl group to the *meta* position led to loss of PDE5 inhibitory activity (compound **a30**). The higher activity displayed by the *ortho*-substituted compound **a29** (IC_{50} = 0.33 μM) might be explained by an intra-molecular H-bond with the imine nitrogen, which stabilizes the coplanar, biologically active conformation, besides its electron-donating effect. This is supported by the 10-fold lower activity noted for the 2-methoxy congener **a13**, which is expected to stabilize a non-coplanar conformation due to the *ortho* effect. In agreement, some of the activity was recovered by positioning the methoxy group in *meta* (**a14**, IC_{50} = 1.8 μM), whereas the *para*-methoxy analogue was inactive (**a15**). The latter unfavorable effect was also apparent in the 3,4-dimethoxy-substituted derivative, strongly suggesting a steric clash of the *para* methyl ether, similar to the methylene bridge in the

https://doi.org/10.1021/acs.jmedchem.0c01120
J. Med. Chem. 2021, 64, 4462−4477

Table 1. Inhibition of Recombinant PDE5 (the Carboxylic Acid Derivatives)

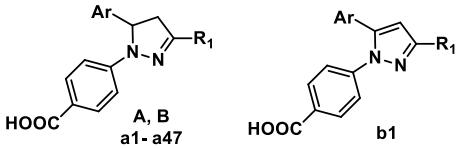

Cpd #	Ar	R1	PDE5 IC_{50} (μM)[a]	Cpd #	Ar	R1	PDE5 IC_{50} (μM)[a]
A	4-tolyl	*t*-Bu	8.4	**a25**	4-methoxyphenyl	4-bromophenyl	ND
B	4-methoxyphenyl	*t*-Bu	2	**a26**	4-methoxyphenyl	*o*-tolyl	0.5
a1	4-methoxyphenyl	cyclopropyl	ND	**a27**	4-methoxyphenyl	*m*-tolyl	1.56
a2	4-methoxyphenyl	1-methylcyclopropyl	ND	**a28**	4-methoxyphenyl	*p*-tolyl	ND
a3	4-methoxyphenyl	cyclohexyl	ND	**a29**	4-methoxyphenyl	2-hydroxyphenyl	0.33
a4	4-methoxyphenyl	phenyl	1.2	**a30**	4-methoxyphenyl	3-hydroxyphenyl	ND
a5	4-methoxyphenyl	pyrrol-2-yl	ND	**a31**	4-methoxyphenyl	4-hydroxyphenyl	2.5
a6	4-methoxyphenyl	pyridin-2-yl	ND	**a32**	4-methoxyphenyl	2-ethoxyphenyl	ND
a7	4-methoxyphenyl	thiophen-2-yl	ND	**a33**	4-methoxyphenyl	4-ethoxyphenyl	ND
a8	4-methoxyphenyl	furan-2-yl	ND	**a34**	4-methoxyphenyl	2-nitrophenyl	ND
a9	4-methoxyphenyl	napthalen-1-yl	ND	**a35**	3-fluoro-4-methoxyphenyl	phenyl	1.19
a10	4-methoxyphenyl	4-phenoxyphenyl	ND	**a36**	3-fluoro-4-methoxyphenyl	*o*-tolyl	0.13
a11	4-methoxyphenyl	[1,1′-biphenyl]-4-yl	ND	**a37**	3-fluoro-4-methoxyphenyl	*t*-Bu	0.59
a12	4-methoxyphenyl	benzo[*d*][1,3]dioxol-5-yl	ND	**a38**	4-trifluoromethylphenyl	*t*-Bu	ND
a13	4-methoxyphenyl	2-methoxyphenyl	3.2	**a39**	4-trifluoromethoxyphenyl	*t*-Bu	10
a14	4-methoxyphenyl	3-methoxyphenyl	1.8	**a40**	4-fluoro-3-methoxyphenyl	*t*-Bu	10.08
a15	4-methoxyphenyl	4-methoxyphenyl	ND	**a41**	3-chloro-4-methoxyphenyl	*t*-Bu	0.9
a16	4-methoxyphenyl	3,4-dimethoxyphenyl	6.9	**a42**	3,5-difluoro-4-methoxyphenyl	*t*-Bu	0.09
a17	4-methoxyphenyl	2-fluorophenyl	ND	**a43**	2,3-difluoro-4-methoxyphenyl	*t*-Bu	0.06
a18	4-methoxyphenyl	3-fluorophenyl	ND	**a44**	2,5-difluoro-4-methoxyphenyl	*t*-Bu	10
a19	4-methoxyphenyl	4-fluorophenyl	3.1	**a45**	3,5-difluorophenyl	*t*-Bu	ND
a20	4-methoxyphenyl	2-chlorophenyl	ND	**a46**	3-fluoro-4-methylphenyl	*t*-Bu	ND
a21	4-methoxyphenyl	3-chlorophenyl	ND	**a47**	3,5-difluoro-4-ethoxyphenyl	*t*-Bu	0.2
a22	4-methoxyphenyl	4-chlorophenyl	ND	**b1**	4-methoxyphenyl	phenyl	ND
a23	4-methoxyphenyl	2,4-dichlorophenyl	ND	sildenafil			0.003
a24	4-methoxyphenyl	2-bromophenyl	ND	celecoxib			37

[a]Full-length PDE5 was used. Values are mean of at least two experiments; standard deviation, <10%; ND: not determined for compounds that showed less than 50% inhibition at 10 μM, no IC_{50} was determined.

Table 2. Inhibition of Recombinant PDE5 (the Rigidified Compounds)

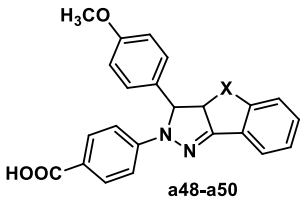

Cpd #	X	PDE5 IC_{50} (μM)[a]
a48	$-CH_2-$	1.44
a49	$-CH_2CH_2-$	ND
a50	$-O-CH_2-$ (O next to Ph)	1.16

[a]Full-length PDE5 was used. Values are mean of at least two experiments; standard deviation, <10%; ND: not determined for compounds that showed less than 50% inhibition at 10 μM, no IC_{50} was determined.

benzodioxolyl derivative **a16** (cf. above). Thus, the exploration of the phenyl binding subpocket using different substituents (also cf. below the *para*-methyl derivative **a28**) showed that its ligand-accessible depth corresponded exactly to the diameter of a phenyl ring. Accordingly, ethoxy substitutions at the *ortho* and *para* positions in compounds **a32** and **a33**, respectively, further diminished the PDE5 inhibitory activity, which may be due to the increased steric requirements. This was apparent by comparing the *ortho*-ethoxy analogue **a32** to the *ortho*-methoxy congener **a13**.

Searching for a replacement of the potentially metabolically problematic *ortho*-OH group in compound **a29**, we synthesized the *ortho*-tolyl derivative, **a26**. Methyl offered electron-donating properties, while a pronounced *ortho*-effect against the five-membered pyrazoline ring was avoided due to the smaller size compared to the methoxy. Indeed, the activity of **a26** (IC_{50} = 0.5 μM) was only slightly reduced compared with that of **a29** and was superior to those of **a27** and **a28** (Table 1).

Confirming the deleterious effect of the electron-withdrawing halogen substituents at the *ortho* position of the 3-phenyl ring, a replacement of the *ortho* electron-donating substituents in the sub-micromolar inhibitors **a26** and **a29** by a nitro group abolished the activity (compound **a34**).

Rigidification of the Structure. As the final stage of optimization at the 3-phenyl, we wanted to explore whether a rigidification of compound **a26** could increase PDE5 inhibitory potency by fixing the dihedral angle between the pyrazoline and the 3-phenyl. Such a strategy seemed straightforward based on the favorable effect of the *ortho*-hydroxy function in **a29**. However, the activity of the conformationally restricted analogue (**a48**) was not enhanced compared to the plain

https://doi.org/10.1021/acs.jmedchem.0c01120
J. Med. Chem. 2021, 64, 4462−4477

Table 3. Inhibition of Recombinant PDE5 (the Amide Derivatives)

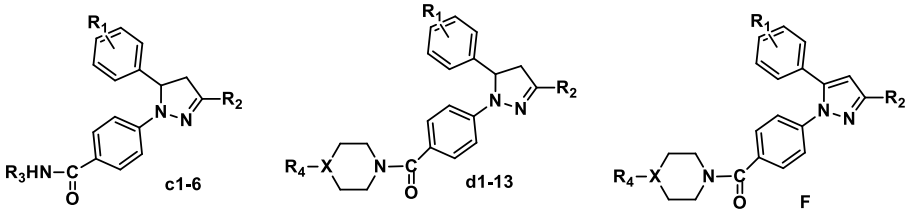

Cpd #	R_1	R_2	R_3	R4	X	PDE5 IC_{50} (μM)[a]
c1	4-methoxy	phenyl	*n*-butyl			0.41
c2	4-methoxy	phenyl	ethyl			0.6
c3	4-methoxy	*t*-Bu	*n*-butyl			1.2
c4	3-fluoro-4-methoxy	*t*-Bu	*n*-butyl			0.41
c5	4-methoxy	*o*-tolyl	*n*-butyl			0.28
c6	4-methoxy	*o*-tolyl	2-hydroxyethyl			0.34
d1	4-methoxy	phenyl		methyl	N	0.078
d2	4-methoxy	*o*-tolyl			O	0.029
d3	4-methoxy	*o*-tolyl		methyl	N	0.021
d4	3-fluoro-4-methoxy	*o*-tolyl		methyl	N	0.04
d5	3-fluoro-4-methoxy	*t*-Bu		methyl	N	0.02
d6	4-fluoro-3-methoxy	*t*-Bu		methyl	N	1.29
d7	3-chlro-4-methoxy	*t*-Bu		methyl	N	0.19
d8	2,3-difluoro-4-methoxy	*t*-Bu		methyl	N	0.004
d9	3,5-difluoro-4-ethoxy	t-Bu		methyl	N	0.13
d10	3-fluoro-4-methyl	*t*-Bu		methyl	N	ND
d11	4-methoxy	*t*-Bu		methyl	N	0.09
d12	3,5-difluoro-4-methoxy	*t*-Bu		methyl	N	0.001
d13	2,5-difluoro-4-methoxy	*t*-Bu		methyl	N	0.26
F	3,5-difluoro-4-ethoxy	*t*-Bu		methyl	N	ND

[a]Full-length PDE5 was used. Values are mean of at least two experiments; standard deviation, <10%; ND: not determined, for compounds that showed less than 50% inhibition at 10 μM, no $IC_{50}$was determined.

phenyl derivative **a4** (Table 2). This result suggested that any entropic advantage due to the restriction of the rotational freedom was countered by a negative effect, which may have resulted from a less favorable fitting of the phenyl into the pocket, since its orientation was shifted by the steric constraints of the five-membered central ring. Increasing the central ring system by one carbon (compound **a49**) led to a significant drop in PDE5 inhibitory potency, which might be explained by a steric collision of the two CH_2 units of the central six-membered ring with the binding cleft. It is also conceivable that the non-polar methylene units did not complement well within the hydrophilic patch in the binding site. The latter hypothesis was supported by our observation that the oxygen-containing isostere of compound **a49** was able to restore the PDE5 inhibitory activity (compound **a50**), which might be due to additional polar interactions offered by the oxygen. However, none of the rigidified analogues showed a significant improvement in the potency. Hence, the non-rigidified, sub-micromolar inhibitor **a26**, with the 3-*o*-tolyl group, was selected for further optimization as it will be discussed below (Figure 2).

Influence of the Chirality of C5. Before we proceeded further in compounds' optimization, we examined the influence of the stereochemistry on the PDE5 inhibitory activity, where chiral separation was made for the sub-micromolar inhibitor compound **a29** obtained from structural variations at the 3-phenyl. The racemic derivative was separated into its respective enantiomers by semi-preparative chiral HPLC. As indicated in Table S2 (Supporting Information), the difference between the IC_{50} values of the separated enantiomers (isomers 1 and 2) was not substantial, suggesting that both enantiomers contribute almost equally to the biological activity of the racemates.

In summary, the most optimal substituents at the 3-position of the pyrazoline regarding PDE5 inhibition were the unsubstituted phenyl (compound **a4**) and a phenyl with small electron-donating group in the *ortho* position (compounds **a26** and **a29**), or a *t*-butyl (compound **B**).

Modification at 5-Phenyl. Compound **B** was also optimized at the 5-phenyl residue. Replacement of the *para*-methoxy substituent by the strong electron-withdrawing 4-trifluoromethyl abolished the activity (compound **a38**). However, the use of the less electron-withdrawing trifluoromethoxy (compound **a39**) partially restored the activity, suggesting the importance of the availability of methoxy electrons and a potential role of methoxy oxygen either as HBA or through its +M mesomeric effect to the 5-phenyl. Adding an adjacent *meta*-fluoro group to the methoxy in compound **B** led to compound **a37** (IC_{50} = 0.59 μM) with about 3-fold increase in potency (**a37** compared to compound **B**), which could be attributed to a direct lipophilic or dipole−dipole interaction mediated by the introduced fluorine atom. Surprisingly, inverting the substitution pattern at the 5-phenyl in **a37** led to more than a 17-fold decrease in PDE5 inhibitory potency by the positional isomer (**a40**), confirming the optimum positioning of both the fluoro and the methoxy substituents in **a37**. Replacing the *meta*-fluoro in **a37** by a chloro substituent gave compound **a41**, which showed slightly reduced PDE5 inhibitory potency (compared to **a37**), indicating that the

https://doi.org/10.1021/acs.jmedchem.0c01120
J. Med. Chem. 2021, 64, 4462−4477

Table 4. Activity and Selectivity of Some Key Compounds on PDE Isoforms[a]

PDE isoform	cpd **c6** IC_{50} (μM)	cpd **d3** IC_{50} (μM)	cpd **d4** IC_{50} (μM)	cpd **d8** IC_{50} (μM)	cpd **d12** IC_{50} (μM)
PDE1A cAMP	>10	>10	>10	>10	>10
PDE1A cGMP	>10	>10	>10	>10	>10
PDE2A cAMP	>50	9.54	>10	>10	>10
PDE2A cGMP	>50	13.34	>10	>10	>10
PDE3A cAMP	>10	>10	>10	>10	>10
PDE3A cGMP	>10	>10	>10	>10	>10
PDE4B2 (cAMP)	>10	>10	>10	>10	>10
PDE5A cGMP	0.34	0.021	0.040	0.004	0.001
PDE6C cGMP	>10	>10	>10	>10	>10
PDE7A (cAMP)	>10	>10	>10	>10	>10
PDE8A (cAMP)	>10	>10	>10	>10	>10
PDE9A cGMP	>10	>10	>10	>10	>10
PDE10A cAMP	>100	32.3	>10	>10	>10
PDE10A cGMP	>100	49.5	>10	>10	>10
PDE11A cAMP	13.03	12.73	>10	>10	>10
PDE11A cGMP	13.04	11.38	>10	>10	>10
IC_{50} ratio PDE6/5	>29	>476	>250	>2500	>10,000
IC_{50} ratio PDE11/5 (cGMP)	38.35	574	>250	>2500	>10,000

[a]Values are mean of at least two experiments; standard deviation, <15%

higher electronegativity of fluorine is more crucial for the activity than the higher lipophilicity of chlorine.

The next step to optimize **a37** (with 3-fluoro-4-methoxy) was to add a second *meta*-fluoro to give either the 3,5- or the 2,3-difluoro-4-methoxy derivative, compounds **a42** and **a43**, respectively. The second fluorine markedly enhanced the potency by 6- and 10-fold, respectively, compared with the mono-fluorinated analogue, **a37** (Table 1). Interestingly, the 2,5-difluoro-4-methoxy isomer (**a44**), carrying the fluorine substituents at opposite positions at the benzene ring, showed a more than 16-fold lower activity (compound **a44** compared to **a37**). The importance of the 4-methoxy as an essential element to generate high potency in combination with fluorine atoms was further confirmed by compounds **a45**−**a47**, where deletion of the 4-methoxy and maintaining the 3,5-difluoro abolished the activity (compound **a45** compared to **a42**). In compound **a46**, the methoxy was replaced by methyl, which has similar electron-donating ability but lacks the +M mesomeric effect and the ability to act as HBA. The methyl group failed to replace the methoxy in compound **a37**, confirming that the methoxy at position 4 is essential for high potency (**a46** compared to **a37**). Finally, replacing the 4-methoxy in compound **a42** with 4-ethoxy (compound **a47**) halved the activity, which can be explained by the higher steric demand of the ethoxy group. Relative to the original hit compounds **B** (IC_{50} = 2 μM), potency optimization through the 5-phenyl was achieved by maintaining the electron-donating methoxy group at the *para* position and adding difluoro substituents to yield **a42** and **a43** (IC_{50} values of 0.09 and 0.06 μM, respectively), demonstrating that multiple fluorination improved the PDE5 inhibitory potency of the hit compound, **B**, up to 33-fold.

Second Round of Optimization: Extension of the Structure through the Modification at the 1-Phenyl. Although a several-fold increase in potency had been achieved, none of the previous modifications could reach single-digit nanomolar potency comparable to marketed PDE5 inhibitors such as sildenafil or tadalafil. To achieve higher potency, it appeared reasonable to extend the structure to establish additional interactions within the binding pocket and greater occupation within the pocket. This extension was achieved through the carboxylic acid moiety at the 1-phenyl.

This strategy was started by the synthesis of several carboxamide derivatives of compound **a26** (a sub-micromolar inhibitor obtained through optimization of the 3-position of pyrazoline). It was encouraging that the *n*-butylamide analogue (compound **c5**) showed a 2-fold increase in potency. To further verify the effect of side chain amides on potency, similar open-chain amide derivatives were prepared for other carboxylic acid analogues like the hit compound **B**, **a4**, or **a37**. The synthesized ethyl or butyl amide derivatives showed about 2-fold increase in potency (compounds **c1**−**c4**). Using a more polar amide side chain, like the 2-hydroxyethyl in compound **c6**, slightly enhanced the potency, indicating that polar side chain amides could be tolerated by this part of the pocket (**c6** compared to **a26**). A synopsis of the SAR obtained with **c1**−**c4** and **c6** suggested that the morpholine heterocycle could be a logical continuation of this series. Indeed, morpholine in compound **d2** (IC_{50} = 0.029 μM) led to a major increase in potency by 12-fold (**d2** compared to compound **c6**). Probably, the morpholine provided the right balance between lipophilicity and polarity, along with a conformational restriction. Then, at one of the last stages of optimization, it was straightforward to replace the morpholine by the dimensionally and electronically related *N*-methylpiperazine (compound **d3**). This modification kept the high level of potency with a slightly lower IC_{50} of 0.021 μM (Figure 2). Thus, converting the carboxyl at the 1-phenyl into the *N*-methylpiperazinylcarbonyl side chain caused a more than 23-fold increase in potency (**d3** compared to **a26**) while also improving the water solubility and drug-like properties.

Third Round of Optimization: Combining Favorable Features. To further optimize PDE5 inhibitory potency, we combined the *N*-methylpiperazinylcarbonyl side chain at the 1-phenyl with the fluorinated 4-methoxyphenyl at position 5 of the pyrazoline while maintaining the *t*-Bu at position 3. This was achieved by reacting compounds **a37**, **a42**, and **a43** with *N*-methylpiperazine; thus, the most potent inhibitors among the series were obtained, namely, compounds **d5**, **d8**, and **d12**, displaying IC_{50} values of 0.020, 0.004, and 0.001 μM,

https://doi.org/10.1021/acs.jmedchem.0c01120
J. Med. Chem. 2021, 64, 4462−4477

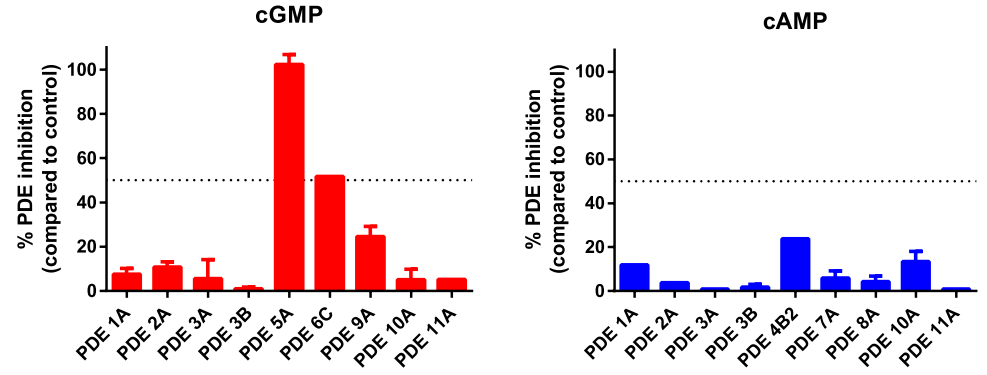

Figure 3. PDE5 isozyme selectivity of compound **d12**. Inhibition of PDE isozymes by compound **d12** at 15 μM (15,000-fold higher concentration than the PDE5 IC_{50} value).

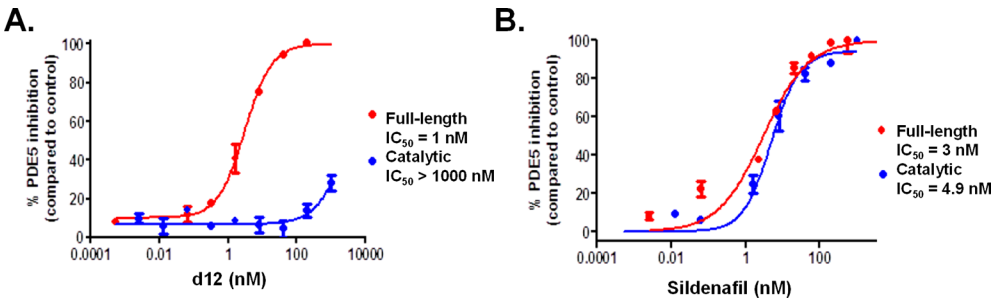

Figure 4. (A) **d12** potently inhibits the full-length PDE5 but not the catalytic fragment. (B) Sildenafil inhibition of the full-length PDE5 and the catalytic fragment as shown in Figure 1 for comparison.

respectively (Table 3). Remarkably, the most potent inhibitor, **d12**, was three times more potent than sildenafil. Thus, combining the features that increased the potency at the 1- and the 5-phenyl proved to be a successful strategy toward more potent PDE5 inhibitors; particularly, the *N*-methylpiperazinyl-carbonyl side chain achieved an up to 90-fold improvement when it was incorporated in the carboxyl precursor compound (compare, e.g., **a42** and **d12**, possessing IC_{50} values of 0.09 and 0.001 μM, respectively). In another series of derivatives, the favorable feature in compound **a26**, namely, the 3-*o*-tolyl, was combined with the 5-(3-fluoro-4-methoxyphenyl) moiety, which was found to be favorable for compound a**37**. The resulting compound **a36** (IC_{50} = 0.13 μM) showed more than 3-fold improvement in potency compared to compound **a26**. However, adding the third feature to **a36** by its reaction with *N*-methylpiperazine to give the amide derivative only led to 3-fold increase in potency (**d4** compared to **a36**), indicating that combining the structural features at positions 1, 3, and 5 of the pyrazoline was not additive. Table S3 (Supporting Information) shows the fold increase in potency after synthesizing amides with *N*-methylpiperazine from some selected carboxylic acid derivatives.

Core Ring: Pyrazole vs Pyrazoline. The importance of the non-coplanar pyrazoline system for PDE5 inhibitory activity was confirmed at different stages of optimization by the oxidation of compounds **a4** and **d9** to the corresponding pyrazole analogues using DDQ to yield compounds **b1** and **F**, respectively. None of the pyrazole analogues showed significant PDE5 inhibition at 10 μM. The abolishment of the core ring planarity in the pyrazoline derivatives with the resulting change in the orientation of the 5-aryl substituent appeared to be an essential requirement for PDE5 inhibitory activity.

PDE Isoform Selectivity. Compound **c6** and the more potent **d3**, **d4**, **d8**, **and d12** were evaluated for their PDE isozyme selectivity using recombinant human PDE isozymes PDE1−PDE11, as summarized in Table 4. The moderately active compound **c6**, but also the highly potent PDE5 inhibitors, **d3**, **d4**, **d8**, and **d12**, showed high selectivity for inhibiting PDE5 with IC_{50} values in the nanomolar range, while the IC_{50} values against all other PDE isozymes were greater than 10 μM. Compound **d12**, the most potent PDE5 inhibitor among the present series, showed unprecedented PDE5 isozyme selectivity. With a selectivity index of >10,000, compound **d12** would be expected to lack the common side effects associated with the classical PDE5 inhibitors such as sildenafil and tadalafil that non-selectively inhibit other PDE isoforms, namely, PDE6 and PDE11, respectively. The excellent PDE isozyme selectivity profile of compound **d12** may be attributed to the unique mode of action that was also found for celecoxib (see below). To confirm the PDE isozyme selectivity of compound **d12**, we screened the compound against all PDE isoforms at a concentration of 15 μM (15,000 times the PDE5 IC_{50}), as shown in Figure 3. Even at this extremely high concentration, compound **d12** only cross-reacted with PDE6 (the closest isoform to PDE5), resulting in approximately 50% inhibition of activity. By comparison, sildenafil has been reported to inhibit PDE6 with IC_{50} values approximately 7-fold higher than IC_{50} values to inhibit PDE5, which accounts for side effects such as visual disturbances.[31] In addition, tadalafil inhibits PDE11 with an IC_{50} value 5-fold higher than the IC_{50} to inhibit PDE5,[31] although the significance of this cross-reactivity is not well known. Thus, to the best of our knowledge, compound **d12** represents the most selective PDE5 inhibitor published to date.

https://doi.org/10.1021/acs.jmedchem.0c01120
J. Med. Chem. 2021, 64, 4462−4477

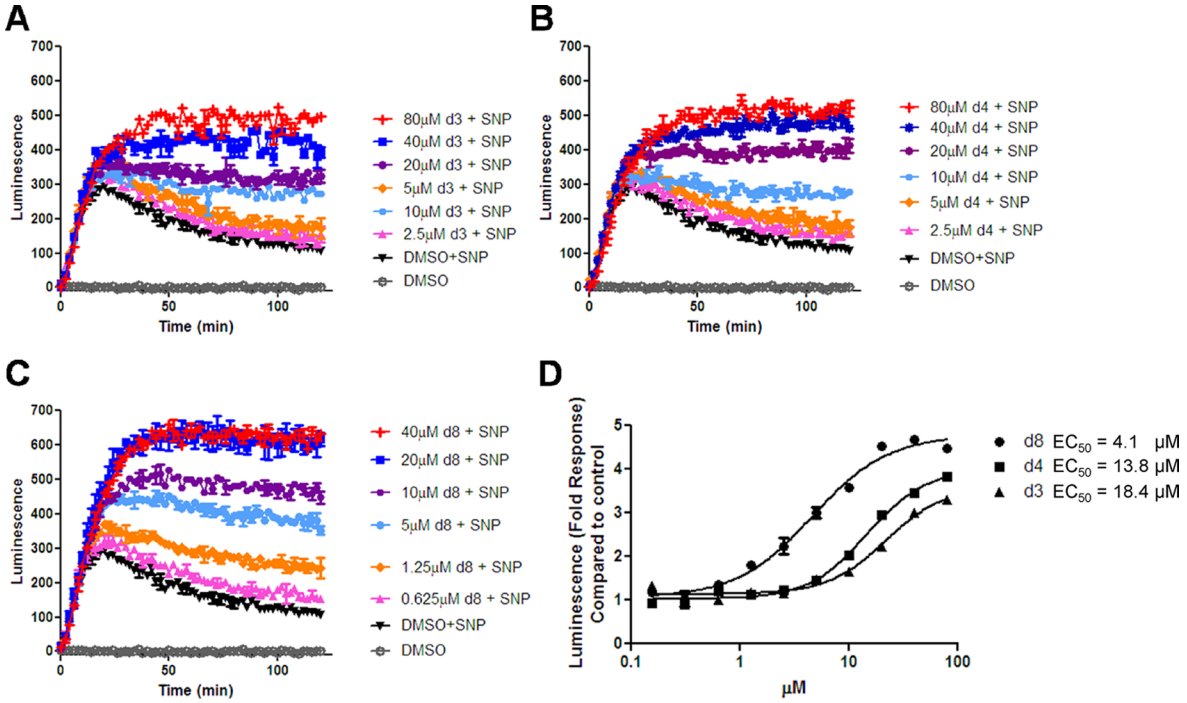

Figure 5. cGMP elevation by **d3**, **d4**, and **d8** in live HEK-293 cells transfected to stably express a cGMP biosensor. The biosensor consists of the PDE5 GAF-A domain fused to a modified firefly luciferase. Intracellular cGMP levels were stimulated with the guanylyl cyclase activator, SNP, at the time of treatment to assess the amplifying effect of a PDE5 inhibitor. Luminescence is therefore an indicator of intracellular cGMP levels. A dose-dependent increase in luminescence was seen when cells were treated with (A) **d3**, (B) **d4**, or (C) **d8**. After 90 min of treatment, a dose-dependent increase was seen. Background luminescence was subtracted, and data were normalized to the DMSO+SNP control. (D) Dose–response curves after a 90 min treatment and the corresponding EC_{50} values.

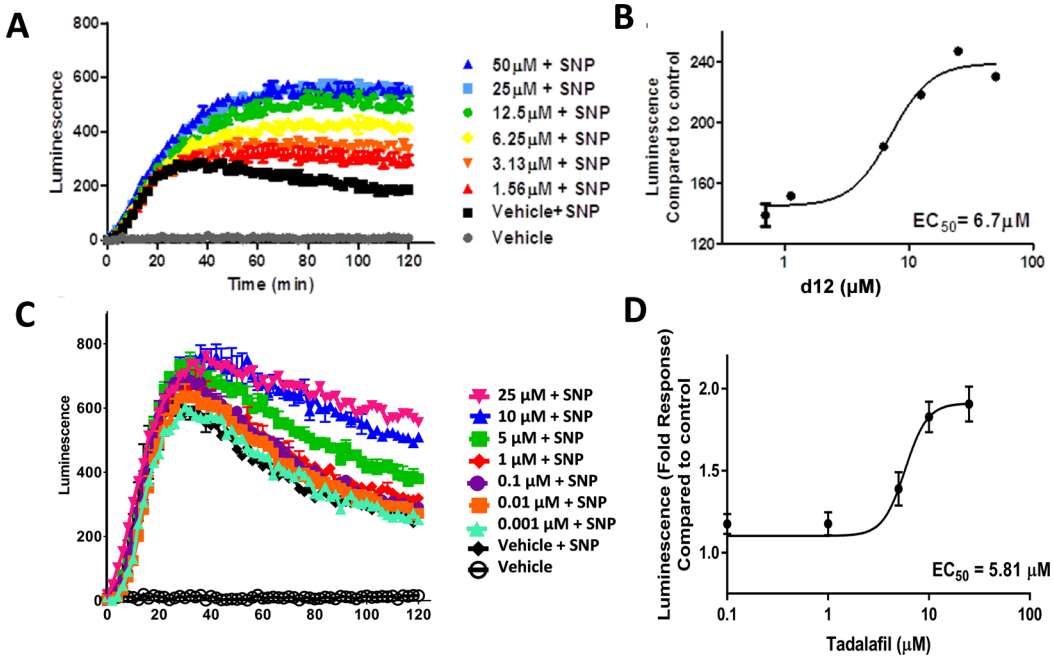

Figure 6. cGMP elevation by **d12** and tadalafil in the cGMP-biosensor assay. A dose-dependent increase in cGMP levels by (A) **d12** and (C) tadalafil. After 90 min of treatment, a dose-dependent increase was observed with (B) **d12** and (D) tadalafil.

Mechanism of PDE5 Inhibition. To determine if the optimized compounds show the same type of dependency on the presence of the regulatory domain as we observed for celecoxib, compound **d12** (IC_{50} = 0.001 μM against full-length enzyme), the most potent compound in the presented series, was tested against the PDE5 catalytic domain along with sildenafil for comparison. As shown in Figure 4, compound **d12** failed to reach the IC_{50} against the PDE5 catalytic domain even at concentrations reaching 1 μM (1000-fold the IC_{50} on the full-length enzyme), while sildenafil inhibited activity with an IC_{50} of 5 nM. These results clearly indicate that the action of compound **d12** strongly depends on the presence of

https://doi.org/10.1021/acs.jmedchem.0c01120
J. Med. Chem. 2021, 64, 4462–4477

regulatory domain, even to a much higher extent than reported previously for vardenafil.[27] To further investigate the mode of action, we studied the enzyme kinetics of **d12** along with sildenafil. In comparison to sildenafil, which is a purely substrate competitive inhibitor, the apparent K_m of **d12** increased only slightly with rising inhibitor concentrations, ruling out a purely competitive mode of inhibition for **d12** (Figure S1, Supporting Information). This was in accordance with the observation that regions outside the catalytic domain provided a major contribution to binding. However, there was no clear tendency toward a non- or uncompetitive mode of inhibition; most likely, **d12** has a mixed mode of inhibition, with a preferred binding to the apo enzyme, while it can also bind to the substrate-bound form, both enabled by the high basal affinity to the adjacent regulatory domain. Hence, the binding site might be located in the interface between the active site and the GAF-B domain. Alternatively, allosteric binding to the regulatory domain with allosteric modulation of the active site would also be in agreement with our experimental findings. At any rate, targeting of non-active site regions, which are mostly less conserved, may explain the unique PDE isozyme selectivity profile of **d12**.

Inhibition of PDE5 in Cells. To determine if PDE5 inhibition and the consequent cGMP elevation occur in treated cells, a cGMP biosensor assay was developed and used to measure changes in intracellular levels of cGMP in living cells in response to treatment with compounds **d3**, **d4**, **d8**, and **d12** along with tadalafil. The four compounds showed a dose-dependent increase in cGMP in HEK-293 cells stably transfected with the cGMP biosensor (Figures 5 and 6). Thus, the ability of the compounds to inhibit PDE5 and increase the intracellular cGMP in live cells was demonstrated. Generally, the compounds showed a similar rank in their cellular potency compared to the rank of their cell-free potency, as can be indicated by the calculated EC_{50} values to increase intracellular cGMP levels after 90 min of treatment of cells with the compounds (Figures 5 and 6). For the two most potent compounds in the present series (**d8** and **d12**), compound **d8** (EC_{50} = 4.13 μM) showed higher efficacy than **d12** in cells (EC_{50} = 6.7 μM).

In Vitro and In Vivo Pharmacokinetic Evaluation and Tolerance Study. We characterized some key pharmacokinetic properties. The intrinsic clearance of **d12** was measured using human hepatic liver microsomes along with terfenadine (rapidly metabolized), imipramine, and propranolol (relatively stable) as reference compounds. Although compound **d12** displayed higher stability than terfenadine, it had a significantly shorter half-life than imipramine and propranolol (Table 5).

Additionally, the binding to human plasma protein was measured using an equilibrium dialysis technique to separate the fraction of a test compound that is unbound from the protein bound fraction. Acebutolol, quinidine, and warfarin are tested in the assay as reference compounds, which yield protein binding values that represent low, medium, and high bindings to human plasma proteins, respectively. Compound **d12** elicited high plasma protein binding with 98% (Table 6).

Preliminary studies were conducted to determine if **d12** reaches systemic circulation after oral administration and if repeated dosing is tolerated. As shown in Figure 7 and in Table 7, after a single oral administration of a dose of 150 mg/kg, **d12** reached a C_{max} of 3995 ng/mL in 2 h (t_{max}) and showed a half-life of 2.3 h. This elimination half-life is in a favorable range for a drug aiming at the treatment of erectile dysfunction.

Table 5. Intrinsic Clearance (Liver Human Microsomes)[a]

compound	half-life (min)	Cl_{int} (μL/min/mg)
d12	22	320.4
terfenadine	11	616.9
imipramine	>60	<115.5
propranolol	>60	<115.5

[a]The test compound (1 μM) was pre-incubated with pooled human liver microsomes (final microsomal protein concentration: 0.1 mg/mL) in phosphate buffer (pH 7.4) for 5 min in a shaking water bath at 37 ° C. The reaction was initiated by adding an NADPH-generating system and incubated for 0, 15, 30, 45, and 60 min. The reaction is stopped by transferring the incubation mixture to acetonitrile/methanol. Samples are then mixed and centrifuged. Supernatants are used for HPLC−MS/MS analysis. The assay was carried out in duplicates, SD < 10%.

Table 6. Binding to Human Plasma Proteins[a]

compound	% protein bound
d12	98
acebutolol	13
quinidine	71
warfarin	99

[a]The samples were dialyzed against phosphate buffered saline (pH 7.4) and the bound and unbound compound fractions quantified by HPLC−MS/MS analysis. The recovery rates were 100% with each compound. Assay was carried out in duplicates, SD < 10%.

Based on the results of the oral PK study, **d12** was reaching the systemic circulation and achieved a C_{max} corresponding to approx. 8.5 μM.

Next, we evaluated the tolerance of **d12** by mice when given twice daily for 28 days (three different doses were used, Figure 8). Twice daily treatment with **d12** by oral gavage was well-tolerated without deaths at all three doses tested. Except for intermittent body weight loss observed in all groups immediately after the start of the treatment (<5% loss from the pre-dose body weight), mice in all three **d12**-treated groups gained weight over the course of the treatment and showed no visible signs of toxicity (Figure 8). The necropsy after termination did not reveal any abnormalities; liver, spleen, and kidney appeared normal upon closer examination. Altogether, these results indicate that **d12** is a promising candidate for in vivo evaluation.

Conclusions. Through systematic rounds of chemical modifications of celecoxib and iterative target-directed screening, we identified a novel series of trisubstituted pyrazolines as potent and selective PDE5 inhibitors that lack COX2 inhibitory activity. The mechanism of inhibition appears to involve binding to the interface region between the regulatory/catalytic domain or to an allosteric site on the regulatory domain, although further research is necessary to fully define the binding site on PDE5. The dependency of the inhibition on the regulatory domain rather than a conserved PDE5 catalytic site may explain the unique selectivity profile of this novel class of PDE5 inhibitors. Altogether, the synthetic strategy presented here led to the development of a new chemotype for PDE5 inhibition with excellent potency and PDE isozyme selectivity, which could be further evaluated in in vivo models. Besides the potential treatment of erectile dysfunction, further indications for **d12** will be explored, such as neuroinflammatory disorders. In a pilot pharmacological study, we obtained preliminary data showing that **d12**

https://doi.org/10.1021/acs.jmedchem.0c01120
J. Med. Chem. 2021, 64, 4462−4477

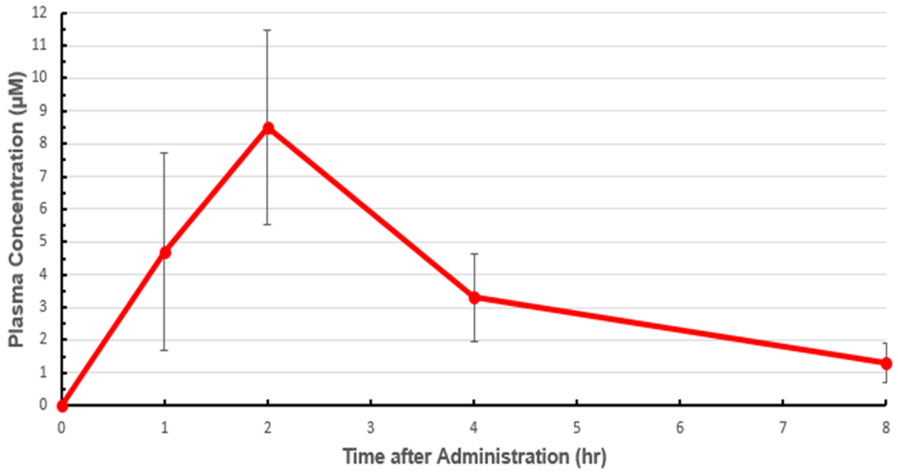

Figure 7. Plasma pharmacokinetics of **d12** in C57BL/6N mice after a single oral administration of a 150 mg/kg dose. Mean ± SD (n = 2−6).

Table 7. Pharmacokinetic Parameters for Compound d12 after Oral Adminstration[a]

PK parameters for **d12**	PO[b]
Ke (1/h)	0.30
$t_{1/2}$ (h)	2.33
t_{max} (h)	2
C_{max} (ng/ml)	3995
$AUC_{0\text{-}8h}$ (ng/ml·h)	14057.5
$AUC_{0\text{-}inf\_obs}$ (ng/ml·h)	16162.1
Vd_{obs} (ml)	625.0
Cl_{obs} (ml/h)	185.6

[a]Ke: elimination rate constant, Vd: volume of distribution, Cl: clearance. [b]A single oral treatment (150 mg/kg) in ethanol/Maalox (10:90, v/v).

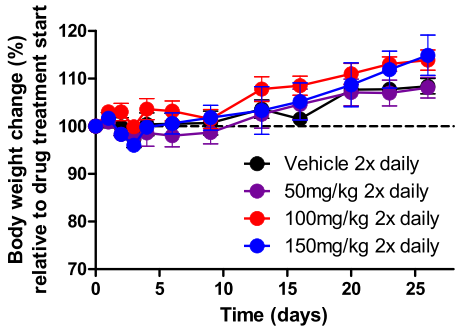

Figure 8. Tolerance of **d12** in mice after chronic oral administration. Body weight change (expressed as percent change from the starting body weight) in athymic nude-Foxn1^{nu} mice over the course of treatment with **d12** administered twice (2×) daily for 28 days by oral gavage. Mean ± SD (n = 4).

was effective in a neuroinflammation model (to be published elsewhere).

EXPERIMENTAL SECTION

Chemistry. Solvents and reagents were obtained from commercial suppliers and used as received. ^{1}H NMR and ^{13}C NMR spectra were measured using an A Bruker DRX 500 spectrometer, and in very few cases, a Varian Mercury VX 300 spectrometer was used for recording the spectra of some enones. The chemical shifts are referenced to the residual protonated solvent signals, and occasionally, TMS was used as a reference. The purity of all the tested compounds (Tables 1−3) was verified by HPLC coupled with mass spectrometry and was at least 95% for all tested compounds. Mass spectra (HPLC−ESI-MS) were acquired using a TSQ quantum (Thermo Electron Corporation) instrument with a triple quadrupole mass detector (Thermo Finnigan) and an ESI source. Samples were introduced using an autosampler (Surveyor, Thermo Finnigan) with an injection volume of 10 μL. The mass detection was determined using a source CID of 10 V and carried out at a spray voltage of 4.2 kV, a nitrogen sheath gas pressure of 4.0 × 10^5 Pa, a capillary temperature of 400 °C, a capillary voltage of 35 V, and an auxiliary gas pressure of 1.0 × 10^5 Pa. The stationary phase used was an RP C18 NUCLEODUR 100-3 (125 × 3 mm) column (Macherey & Nagel). The solvent system consisted of water containing 0.1% TFA (A) and 0.1% TFA in acetonitrile (B). For the HPLC method, the flow rate was 400 μL/min. The percentage of B started at 5%, increased up to 100% over 16 min, kept at 100% for 2 min, and then flushed back to 5% in 2 min. Melting points were determined using a Mettler FP1 melting point apparatus and are uncorrected.

General Synthetic Methods and Experimental Details for Key Compounds. *General Procedure for the Enone Synthesis.* The appropriate ketone (10 mmol) was reacted with corresponding aryl aldehyde (10 mmol) using the same procedure that we previously reported in ref 32.

(*E*)-1-(3,5-Difluoro-4-methoxyphenyl)-4,4-dimethylpent-1-en-3-one (**E42**) was synthesized according to the general procedure for enone synthesis using pinacolone and 3,5-difluoro-4-methoxybenzaldehyde; white solid; yield: 2.44 g (95.9%); mp 74−75 °C;^{1}H NMR (500 MHz, DMSO-d_6) δ 1.15 (s, 9H), 3.97 (t, J = 1.1 Hz, 3H), 7.35−7.50 (m, 2H), 7.62−7.72 (m, 2H); ^{13}C NMR (126 MHz, DMSO-d_6) δ 25.58, 42.9, 61.71 (t, $^4J_{C\text{-}F}$ = 3.4 Hz), 112.68 (dd, $^2J_{C\text{-}F}$ = 17.5, $^4J_{C\text{-}F}$ = 5.8 Hz), 122.91, 130.15 (t, $^3J_{C\text{-}F}$ = 9.3 Hz), 136.94 (t, $^2J_{C\text{-}F}$ = 14.2 Hz), 139.41 (t, $^4J_{C\text{-}F}$ = 2.5 Hz), 154.82 (dd, $^1J_{C\text{-}F}$ = 246.1, $^3J_{C\text{-}F}$ = 6.5 Hz), 203.28.

(*E*)-1-(2,3-Difluoro-4-methoxyphenyl)-4,4-dimethylpent-1-en-3-one (**E43**) was synthesized according to the general procedure for enone synthesis using pinacolone and 2,3-difluoro-4-methoxybenzaldehyde; white solid; yield: 2.34 g (92%); mp 128−129 °C; ^{1}H NMR (500 MHz, DMSO-d_6) δ 1.16 (s, 9H), 3.93 (s, 3H),7.07−7.12 (m, 1H), 7.40 (d, J = 15.8 Hz, 1H), 7.54 (d, J = 15.8 Hz, 1H), 7.77 (td, J = 8.8, 2.2 Hz, 1H); ^{13}C NMR (126 MHz, DMSO-d_6) δ 25.80, 42.77, 56.60, 109.37 (d, $^4J_{C\text{-}F}$ = 2.6 Hz), 116.15 (d, $^2J_{C\text{-}F}$ = 8.9 Hz), 122.39 (d, $^2J_{C\text{-}F}$ = 4.9 Hz), 123.92, 132.81, 140.08 (dd, $^1J_{C\text{-}F}$ = 245.5, $^2J_{C\text{-}F}$ = 14.4 Hz), 149.42 (dd, $^1J_{C\text{-}F}$ = 251.1, $^2J_{C\text{-}F}$ = 10.5 Hz), 150.01 (dd, $^2J_{C\text{-}F}$ = 7.6, $^3J_{C\text{-}F}$ = 3.5 Hz), 203.10.

General Procedure for the Pyrazoline Synthesis. A mixture of the enone derivative (2 mmol) and the corresponding aryl hydrazine hydrochloride (3 mmol) were reacted together using the same procedure that we previously reported in ref 32.

4-(5-(4-Methoxyphenyl)-3-(*o*-tolyl)-4,5-dihydro-1*H*-pyrazol-1-yl) benzoic acid (**a26**) was prepared by reaction of (*E*)-3-(4-

https://doi.org/10.1021/acs.jmedchem.0c01120
J. Med. Chem. 2021, 64, 4462−4477

methoxyphenyl)-1-(*o*-tolyl) prop-2-en-1-one (**E26**) and 4-hydrazinobenzoic acid hydrochloride according to the general procedure for pyrazoline synthesis. The product was purified by CC (CH_2Cl_2/CH_3OH, 100:0.5); yellow solid; yield: 0.25 g (32.4%); mp 209−210 °C; ^{1}H NMR (500 MHz, DMSO-d_6) δ 2.70 (s, 3H, −Ph−C$\underline{H}_3$), 3.19 (dd, J = 17.4, 5.0 Hz, 1H, $\underline{H}_a$−C4), 3.70 (s, 3H, −OC$\underline{H}_3$), 4.01 (dd, J = 17.4, 12.0 Hz, 1H, $\underline{H}_b$−C4), 5.51 (dd, J = 11.9, 5.0 Hz, 1H, $\underline{H}$−C5), 6.86−6.92 (m, 2H, ArC$\underline{H}$), 6.97−7.03 (m, 2H, ArC$\underline{H}$), 7.16−7.22 (m, 2H, ArC$\underline{H}$), 7.23−7.37 (m, 3H, ArC$\underline{H}$), 7.44−7.47 (m, 1H, ArC$\underline{H}$), 7.71−7.77 (m, 2H, ArC$\underline{H}$), 12.27 (s, 1H, −COO$\underline{H}$); ^{13}C NMR (125 MHz, DMSO-d_6) δ 23.45 (−Ph$\underline{C}H_3$), 45.09 (C4), 55.00 (−O$\underline{C}H_3$), 60.92 (C5), 111.93 (Ar$\underline{C}$H), 114.40 (Ar$\underline{C}$H), 119.81 (Ar$\underline{C}$H), 126.03 (Ar$\underline{C}$H), 126.98 (Ar$\underline{C}$H), 128.49 (Ar$\underline{C}$H), 128.70 (Ar$\underline{C}$H), 130.42 (Ar$\underline{C}$H), 130.79 (Ar$\underline{C}$H), 131.50 (Ar$\underline{C}$H), 133.73 (Ar$\underline{C}$H), 136.72 (Ar$\underline{C}$H), 147.04 (Ar$\underline{C}$H), 150.43 (Ar$\underline{C}$H), 158.55 ($\underline{C}$3═N), 167.20 ($\underline{C}$═O); MS (ESI): m/z = 386.75 (M + H)$^+$.

4-(3-*tert*-Butyl-5-(3-fluoro-4-methoxyphenyl)-4,5-dihydro-1*H*-pyrazol-1-yl)-benzoic acid (**a37**) was prepared by reaction of (*E*)-1-(3-fluoro-4-methoxyphenyl)-4,4-dimethylpent-1-en-3-one (**E37**) and 4-hydrazinobenzoic acid hydrochloride according to the general procedure for pyrazoline synthesis. The product was purified by CC (CH_2Cl_2:CH_3OH, 100:2); white solid; yield: 0.16 g (22%); ^{1}H NMR (500 MHz, DMSO-d_6) δ 1.15 (s, 9H, −C(C$\underline{H}_3$)$_3$), 2.72 (dd, J = 17.8, 5.1 Hz, 1H, $\underline{H}_a$−C4), 3.52 (dd, J = 17.7, 11.7 Hz, 1H, $\underline{H}_b$−C4), 3.76 (s, 3H, −OC$\underline{H}_3$), 5.32 (dd, J = 11.6, 5.0 Hz, 1H, $\underline{H}$−C5), 6.81−6.85 (m, 2H, ArC$\underline{H}$), 6.92 (dd, J = 8.5, 1.4 Hz, 1H, ArC$\underline{H}$), 6.99 (dd, J = 12.2, 2.1 Hz, 1H, ArC$\underline{H}$), 7.08 (t, J = 8.7 Hz, 1H, ArC$\underline{H}$), 7.67−7.73 (m, 2H, ArC$\underline{H}$), 12.19 (s, 1H, −COO$\underline{H}$); ^{13}C NMR (125 MHz, DMSO-d_6) δ 27.84 (−C($\underline{C}H_3$)$_3$), 33.56 (−$\underline{C}$(CH$_3$)$_3$), 42.41 (C4), 55.91 (−O$\underline{C}H_3$), 61.27 (C5), 111.42 (Ar$\underline{C}$H), 113.26 (d, $^2J_{C\text{-}F}$ = 18.6 Hz, Ar$\underline{C}$H), 114.31 (d, $^3J_{C\text{-}F}$ = 1.2 Hz, Ar$\underline{C}$H), 119.15 (Ar$\underline{C}$H), 121.71 (d, $^4J_{C\text{-}F}$ = 3.2 Hz, Ar$\underline{C}$H), 130.78 (Ar$\underline{C}$H), 134.97 (d, $^3J_{C\text{-}F}$ = 5.1 Hz, Ar$\underline{C}$H), 146.28 (d, $^2J_{C\text{-}F}$ = 10.4 Hz, Ar$\underline{C}$H), 147.74 (Ar$\underline{C}$H), 151.46 (d, $^1J_{C\text{-}F}$ = 244.9 Hz, Ar$\underline{C}$H), 161.58 ($\underline{C}$3═ N), 167.27 ($\underline{C}$═O); MS (ESI): m/z = 370.89 (M + H)$^+$.

4-(3-(*tert*-Butyl)-5-(3,5-difluoro-4-methoxyphenyl)-4,5-dihydro-1*H*-pyrazol-1-yl)benzoic acid (**a42**) was prepared by reaction of (*E*)-1-(3,5-difluoro-4-methoxyphenyl)-4,4-dimethylpent-1-en-3-one (**E42**) and 4-hydrazinobenzoic acid hydrochloride according to the general procedure for pyrazoline synthesis. The product was purified by CC (CH_2Cl_2/CH_3OH, 100:2); white solid; yield: 0.53 g (68.3%); mp 222−223 °C; ^{1}H NMR (500 MHz, DMSO-d_6) δ 1.18 (s, 9H, −C(C$\underline{H}_3$)$_3$), 2.80 (dd, J = 17.8, 5.2 Hz, 1H, $\underline{H}_a$−C4), 3.56 (dd, J = 17.8, 11.7 Hz, 1H, $\underline{H}_b$−C4), 3.88 (s, 3H, −OC$\underline{H}_3$), 5.35 (dd, J = 11.7, 5.2 Hz, 1H, $\underline{H}$−C5), 6.87 (d, J = 9.0 Hz, 2H, ArC$\underline{H}$), 6.94 (d, J = 8.9 Hz, 2H, ArC$\underline{H}$), 7.71 (d, J = 9.1 Hz, 2H, ArC$\underline{H}$), 12.24 (s, 1H, −COO$\underline{H}$); ^{13}C NMR (126 MHz, DMSO-d_6) δ 27.79 (−C($\underline{C}H_3$)$_3$), 33.53 (−$\underline{C}$(CH$_3$)$_3$), 42.20 (C4), 61.16 (−O$\underline{C}H_3$), 61.68 (t, $^4J_{C\text{-}F}$ = 2.8 Hz, C5), 109.74 (dd, $^2J_{C\text{-}F}$ = 17.5, $^4J_{C\text{-}F}$ = 5.7 Hz, Ar$\underline{C}$H), 111.46 (Ar$\underline{C}$H), 111.54 (Ar$\underline{C}$H), 119.48 (Ar$\underline{C}$H), 130.87 (Ar$\underline{C}$H), 134.76 (t, $^2J_{C\text{-}F}$ = 14.2 Hz, Ar$\underline{C}$H), 138.14 (t, $^3J_{C\text{-}F}$ = 7.3 Hz, Ar$\underline{C}$H), 147.62 (Ar$\underline{C}$H), 155.18 (dd, $^1J_{C\text{-}F}$ = 247.7, $^3J_{C\text{-}F}$ = 6.1 Hz, Ar$\underline{C}$H), 161.67 ($\underline{C}$3═N), 167.20 ($\underline{C}$═O); MS (ESI): m/z = 389.16 (M + H)$^+$.

4-(3-(*tert*-Butyl)-5-(2,3-difluoro-4-methoxyphenyl)-4,5-dihydro-1*H*-pyrazol-1-yl)benzoic acid (**a43**) was prepared by the reaction of (*E*)-1-(2,3-difluoro-4-methoxyphenyl)-4,4-dimethylpent-1-en-3-one (**E43**) and 4-hydrazinobenzoic acid hydrochloride according to the general procedure for pyrazoline synthesis. The product was purified by CC (CH_2Cl_2/CH_3OH, 100:2); faint yellow solid; yield 0.51 g (65%); mp 204−205 °C; ^{1}H NMR (500 MHz, DMSO-d_6) δ 1.18 (s, 9H, −C(C$\underline{H}_3$)$_3$), 2.86 (dd, J = 17.7, 4.8 Hz, 1H, $\underline{H}_a$−C4), 3.60 (dd, J = 17.7, 11.9 Hz, 1H, $\underline{H}_b$−C4), 3.82 (s, 3H, −OC$\underline{H}_3$), 5.51 (dd, J = 11.9, 4.8 Hz, 1H, $\underline{H}$−C5), 6.79−6.83 (m, 1H, ArC$\underline{H}$), 6.86 (d, J = 9.0 Hz, 2H, ArC$\underline{H}$), 6.94 (q, J = 7.9 Hz, 1H, ArC$\underline{H}$), 7.70 (d, J = 9.0 Hz, 2H, ArC$\underline{H}$), 12.22 (s, 1H, −COO$\underline{H}$); ^{13}C NMR (126 MHz, DMSO-d_6) δ 27.84 (−C($\underline{C}H_3$)$_3$), 33.55 (−$\underline{C}$(CH$_3$)$_3$), 41.11 (C4), 56.28 (−O$\underline{C}H_3$), 56.42 (C5), 109.12 (d, $^3J_{C\text{-}F}$ = 1.5 Hz, Ar$\underline{C}$H), 111.27 (Ar$\underline{C}$H), 119.27 (Ar$\underline{C}$H), 121.23 (t, $^3J_{C\text{-}F}$ = 4.0 Hz, Ar$\underline{C}$H), 121.71 (d, $^2J_{C\text{-}F}$ = 11.9 Hz, Ar$\underline{C}$H), 130.86 (Ar$\underline{C}$H), 140.19 (dd, $^1J_{C\text{-}F}$ = 246.4, $^2J_{C\text{-}F}$ = 14.2 Hz, Ar$\underline{C}$H), 147.49 (Ar$\underline{C}$H), 147.83 (dd, $^2J_{C\text{-}F}$ = 7.2, $^3J_{C\text{-}F}$ = 2.0 Hz, Ar$\underline{C}$H), 147.97 (dd, $^1J_{C\text{-}F}$ = 245.7, $^2J_{C\text{-}F}$ = 10.5 Hz, Ar$\underline{C}$H), 161.84 ($\underline{C}$3═N), 167.22 ($\underline{C}$═O); MS (ESI): m/z = 389.16 (M + H)$^+$.

General Procedure for Amide Synthesis. The appropriate amine (2 equiv) was added to a solution of the respective benzoic acid derivative (1 equiv) and EDCI·HCl (1.5 equiv) in absolute CH_2Cl_2 (10 mL). The mixture was stirred overnight at room temperature and monitored by TLC. After completion of the reaction, the solvent was removed under reduced pressure. The crude product was purified by column chromatography on a silica gel to give the desired product.

N-(2-Hydroxyethyl)-4-(5-(4-methoxyphenyl)-3-(*o*-tolyl)-4,5-dihydro-1*H*-pyrazol-1-yl) benzamide (**c6**) was prepared by reaction of 4-(5-(4-methoxyphenyl)-3-(*o*-tolyl)-4,5-dihydro-1*H*-pyrazol-1-yl) benzoic acid (**a26**) and ethanolamine according to the general procedure for amide synthesis. The product was purified by CC (CH_2Cl_2/CH_3OH, 100:2); faint yellow solid; yield: 0.039 g (9%); mp 68−70 °C; ^{1}H NMR (500 MHz, DMSO-d_6) δ 2.70 (s, 3H, −Ph−C$\underline{H}_3$), 3.18 (dd, J = 17.3, 4.2 Hz, 1H, $\underline{H}_a$−C4), 3.23−3.29 (m, 2H, −C$\underline{H}_2$−), 3.43−3.48 (m, 2H, −C$\underline{H}_2$−),3.70 (s, 3H, −OC$\underline{H}_3$), 3.99 (dd, J = 17.1, 12.5 Hz, 1H, $\underline{H}_b$−C4), 4.68 (s, 1H, −O$\underline{H}$), 5.49 (dd, J = 11.8, 4.9 Hz, 1H, $\underline{H}$−C5), 6.88 (d, J = 8.0 Hz, 2H, ArC$\underline{H}$), 6.97 (d, J = 8.2 Hz, 2H, ArC$\underline{H}$), 7.19 (d, J = 8.1 Hz, 2H, ArC$\underline{H}$), 7.23−7.29 (m, 2H, ArC$\underline{H}$), 7.33 (d, J = 6.3 Hz, 1H, ArC$\underline{H}$), 7.41−7.47 (m, 1H, ArC$\underline{H}$), 7.67 (d, J = 8.4 Hz, 2H, ArC$\underline{H}$), 8.07 (s, 1H, −N$\underline{H}$−); ^{13}C NMR (125 MHz, DMSO-d_6) δ 23.41 (−Ph$\underline{C}H_3$), 41.97 (C4), 45.00 (−$\underline{C}H_2$−), 55.00 (−$\underline{C}H_2$−), 59.94 (−O$\underline{C}H_3$), 61.09 (C5), 111.84 (Ar$\underline{C}$H), 114.33 (Ar$\underline{C}$H), 123.96 (Ar$\underline{C}$H), 126.02 (Ar$\underline{C}$H), 127.07 (Ar$\underline{C}$H), 128.32 (Ar$\underline{C}$H), 128.38 (Ar$\underline{C}$H), 128.56 (Ar$\underline{C}$H), 130.58 (Ar$\underline{C}$H), 131.48 (Ar$\underline{C}$H), 133.87 (Ar$\underline{C}$H), 136.57 (Ar$\underline{C}$H), 145.89 (Ar$\underline{C}$H), 149.66 (Ar$\underline{C}$H), 158.50 ($\underline{C}$3═N), 166.08 ($\underline{C}$═O); MS (ESI): m/z = 429.88 (M + H)$^+$.

(4-(5-(4-Methoxyphenyl)-3-(*o*-tolyl)-4,5-dihydro-1*H*-pyrazol-1yl)-phenyl)(Morpholino) methanone (**d2**) was prepared by reaction of 4-(5-(4-methoxyphenyl)-3-(*o*-tolyl)-4,5-dihydro-1*H*-pyrazol-1-yl) benzoic acid (**a26**) and morpholine according to the general procedure for amide synthesis. The product was purified by CC (CH_2Cl_2/CH_3OH, 100:2); yellow solid; yield: 0.068 g (15%); mp 144−146 °C; ^{1}H NMR (500 MHz, DMSO-d_6) δ 2.70 (s, 3H, −Ph−C$\underline{H}_3$), 3.17 (dd, J = 17.3, 5.7 Hz, 1H, $\underline{H}_a$−C4), 3.46 (s, 4H, −C$\underline{H}_2$−NCO−C$\underline{H}_2$−), 3.56 (t, J = 4.6 Hz, 4H, −C$\underline{H}_2$−O−C$\underline{H}_2$−), 3.71 (s, 3H, −OC$\underline{H}_3$), 3.98 (dd, J = 17.3, 12.0 Hz, 1H, $\underline{H}_b$−C4), 5.43 (dd, J = 12.0, 5.7 Hz, 1H, $\underline{H}$−C5), 6.88−6.92 (m, 2H, ArC$\underline{H}$), 6.97−7.01 (m, 2H, ArC$\underline{H}$), 7.29−7.23 (m, 2H, ArC$\underline{H}$), 7.24−7.30 (m, 4H, ArC$\underline{H}$),7.31−7.35 (m, 1H, ArC$\underline{H}$), 7.41−7.45 (m, 1H, ArC$\underline{H}$); ^{13}C NMR (125 MHz, DMSO-d_6) δ 23.49 (−Ph$\underline{C}H_3$), 40.10 (C4), 45.15 (−$\underline{C}H_2$−), 55.00 (−$\underline{C}H_2$−), 61.27 (−O$\underline{C}H_3$), 66.11 (C5), 111.95 (Ar$\underline{C}$H), 114.41 (Ar$\underline{C}$H), 124.53 (Ar$\underline{C}$H), 126.01 (Ar$\underline{C}$H), 127.03 (Ar$\underline{C}$H), 128.26 (Ar$\underline{C}$H), 128.55 (Ar$\underline{C}$H), 128.90 (Ar$\underline{C}$H), 130.56 (Ar$\underline{C}$H), 131.47 (Ar$\underline{C}$H), 134.06 (Ar$\underline{C}$H), 136.57 (Ar$\underline{C}$H), 145.15 (Ar$\underline{C}$H), 149.36 (Ar$\underline{C}$H), 158.53 ($\underline{C}$3═N), 169.32 ($\underline{C}$═O); MS (ESI): m/z = 455.94 (M + H)$^+$.

(4-(5-(4-Methoxyphenyl)-3-(*o*-tolyl)-4,5-dihydro-1*H*-pyrazol-1-yl)phenyl)(4-methylpiperazin-1-yl)methanone (**d3**). The title compound was prepared by reaction of 4-(5-(4-methoxyphenyl)-3-(*o*-tolyl)-4,5-dihydro-1*H*-pyrazol-1-yl)benzoic acid (**a26**) and 1-methylpiperazine according to the general procedure for amide synthesis. The product was purified by CC (CH_2Cl_2/CH_3OH, 100:2); yellow solid; yield: 0.098 g (21%); mp 127−128 °C; ^{1}H NMR (500 MHz, DMSO-d_6) δ 2.28 (s, 3H, N−C$\underline{H}_3$), 2.45 (s, 4H, −C$\underline{H}_2$−NCH$_3$−C$\underline{H}_2$−), 2.69 (s, 3H, −ph-C$\underline{H}_3$), 3.16 (dd, J = 17.4, 5.7 Hz, 1H, $\underline{H}_a$−C4), 3.50−3.55 (m, 4H, −C$\underline{H}_2$−NCO−C$\underline{H}_2$−), 3.70 (s, 3H, −OC$\underline{H}_3$), 3.98 (dd, J = 17.3, 12.0 Hz, 1H, $\underline{H}_b$−C4), 5.42 (dd, J = 11.9, 5.6 Hz, 1H, $\underline{H}$−C5), 6.87−6.90 (m, 2H, ArC$\underline{H}$), 6.96−7.00 (m, 2H, ArC$\underline{H}$), 7.18−7.23 (m, 2H, ArC$\underline{H}$), 7.23−7.29 (m, 4H, ArC$\underline{H}$), 7.30−7.35 (m, 1H, ArC$\underline{H}$), 7.40−7.44 (m, 1H, ArC$\underline{H}$); ^{13}C NMR (125 MHz, DMSO) δ 30.73 (−Ph$\underline{C}H_3$), 35.74 (C4), 45.68 (−N$\underline{C}H_3$), 54.96 (−$\underline{C}H_2$−), 63.46 (−O$\underline{C}H_3$), 66.79 (C5), 111.97 (Ar$\underline{C}$H), 114.30 (Ar$\underline{C}$H), 116.19 (Ar$\underline{C}$H), 117.34 (Ar$\underline{C}$H), 119.67

https://doi.org/10.1021/acs.jmedchem.0c01120
J. Med. Chem. 2021, 64, 4462−4477

(ArCH), 121.70 (ArCH), 124.28 (ArCH), 126.84 (ArCH), 130.88 (ArCH), 131.41 (ArCH), 145.68 (ArCH), 146.36 (ArCH), 155.42 (ArCH), 158.82 (ArCH), 162.26 (C3=N), 167.17 (C=O); MS (ESI): m/z = 469.31 $(M + H)^+$.

(4-(3-(*tert*-Butyl)-5-(2,3-difluoro-4-methoxyphenyl)-4,5-dihydro-1*H*-pyrazol-1-yl)phenyl)(4-methylpiperazin-1-yl)methanone (**d8**) was prepared by reaction of 4-(3-(*tert*-butyl)-5-(2,3-difluoro-4-methoxyphenyl)-4,5-dihydro-1*H*-pyrazol-1-yl)benzoic acid (**a43**) and *N*-methylpiperazine according to the general procedure for amide synthesis. The product was purified by CC (CH_2Cl_2/CH_3OH, 100:5); faint yellow solid; yield: 0.21 g (44.6%); mp 92−93 °C; ^{1}H NMR (500 MHz, DMSO-d_6) δ 1.18 (s, 9H, −C(CH_3)$_3$), 2.17 (s, 3H, N−CH_3), 2.27 (s, 4H, −CH_2−NCH_3−CH_2−), 2.83 (dd, J = 17.7, 5.6 Hz, 1H, H_a−C4), 3.44 (s, 4H, −CH_2−NCO−CH_2−), 3.59 (dd, J = 17.7, 11.9 Hz, 1H, H_b−C4), 3.82 (s, 3H, −OCH_3), 5.40 (dd, J = 12.0, 5.6 Hz, 1H, H−C5), 6.82 (dd, J = 18.6, 8.1 Hz, 2H, ArCH), 6.85−6.90 (m, 1H, ArCH), 6.96 (t, J = 7.9 Hz, 1H, ArCH), 7.19 (t, J = 7.6 Hz, 2H, ArCH); ^{13}C NMR (126 MHz, DMSO-d_6) δ 27.88 (−C(CH_3)$_3$), 33.48 (−C(CH_3)$_3$), 41.14 (C4), 45.59 (−NCH_3), 54.54 (−CH_2−), 56.43 (C5), 56.72 (−OCH_3), 109.18 (ArCH), 111.23 (d, $^3J_{C-F}$ = 8.3 Hz, ArCH), 111.4 (ArCH), 121.30 (dd, $^3J_{C-F}$ = 6.5, $^4J_{C-F}$ = 2.9 Hz, ArCH), 122.14 (d, $^2J_{C-F}$ = 11.3 Hz, ArCH), 124.50 (ArCH), 128.78 (ArCH), 140.18 (dd, $^1J_{C-F}$ = 246.5, $^2J_{C-F}$ = 14.6 Hz, ArCH), 145.75 (ArCH), 147.77 (dd, $^2J_{C-F}$ = 7.8, $^3J_{C-F}$ = 2.6 Hz, ArCH), 147.95 (dd, $^1J_{C-F}$ = 244.0, $^2J_{C-F}$ = 12.2 Hz, ArCH), 160.68 (C3=N), 169.25 (C=O); MS (ESI): m/z = 471.25 $(M + H)^+$.

(4-(3-(*tert*-Butyl)-5-(3,5-difluoro-4-methoxyphenyl)-4,5-dihydro-1*H*-pyrazol-1-yl)phenyl)(4-methylpiperazin-1-yl)methanone (**d12**) was prepared by reaction of 4-(3-(*tert*-butyl)-5-(3,5-difluoro-4-methoxyphenyl)-4,5-dihydro-1*H*-pyrazol-1-yl)benzoic acid (**a42**) and *N*-methylpiperazine according to the general procedure for amide synthesis. The product was purified by CC (CH_2Cl_2/CH_3OH, 100:5); faint yellow solid; yield: 0.25 g (53.13%); mp 85−86 °C; ^{1}H NMR (500 MHz, DMSO-d_6) δ 1.17 (s, 9H, −C(CH_3)$_3$), 2.17 (s, 3H, N−CH_3), 2.26 (s, 4H, −CH_2−NCH_3−CH_2−), 2.76 (dd, J = 17.7, 6.3 Hz, 1H, H_a−C4), 3.44 (s, 4H, −CH_2−NCO−CH_2−), 3.55 (dd, J = 11.1, 6.6 Hz, 1H, H_b−C4), 3.88 (s, 3H, −OCH_3), 5.23 (dd, J = 11.7, 6.3 Hz, 1H, H−C5), 6.85 (d, J = 8.8 Hz, 2H, ArCH), 6.99 (d, J = 8.9 Hz, 2H, ArCH), 7.21 (d, J = 8.9 Hz, 2H, ArCH); ^{13}C NMR (126 MHz, DMSO-d_6) δ 27.83 (−C(CH_3)$_3$), 33.46 (−C(CH_3)$_3$), 42.31 (C4), 45.59 (−NCH_3), 54.54 (−CH_2−), 61.69 (t, $^4J_{C-F}$ = 2.8 Hz, C5), 61.85 (−OCH_3), 109.80 (dd, $^2J_{C-F}$ = 17.7, $^4J_{C-F}$ = 5.5 Hz, ArCH), 111.67 (ArCH), 111.76 (ArCH), 124.77 (ArCH), 128.76 (ArCH), 134.72 (t, $^2J_{C-F}$ = 14.2 Hz, ArCH), 138.59 (t, $^3J_{C-F}$ = 7.3 Hz, ArCH), 145.95 (ArCH), 155.20 (dd, $^1J_{C-F}$ = 247.5, $^3J_{C-F}$ = 6.0 Hz, ArCH), 160.57 (C3=N), 169.21 (C=O); MS (ESI): m/z = 471.25 $(M + H)^+$.

General Procedure for Pyrazoline Oxidation to Pyrazole. A mixture of the pyrazoline derivative (1 mmol) and DDQ (1.5 mmol) in 10 mL of benzene was heated to reflux for 5 h. The mixture was cooled to room temperature and filtered through a plug of silica gel wetted with diethyl ether. The filtrate was concentrated *in vacuo*, and the residue was purified by CC.

Phosphodiesterase Assay. Recombinant GST-tagged phosphodiesterase enzymes purified from baculovirus infected sf9 cells were purchased from BPS Bioscience (PDE1A full length, PDE2A full length, PDE3A [669-end], PDE3B [592-end], PDE4B2 full length, PDE5A1 full length, PDE6C full length, PDE7A [122-end], PDE8A1 full length, PDE9A2 full length, PDE10A2 full length, and PDE11A4 full length). Recombinant 6His tagged-PDE5 catalytic domain was purified from *Escherechia coli* using a Talon IMAC column (construct kindly provided by Dr. Hengming Ke at The University of North Carolina at Chapel Hill). Enzyme (5 μg/mL) was added to the wells of black 96-well non-binding plates. Immediately, the protein was treated with compound or vehicle control and 50 nM TAMRA-cGMP or FAM-cAMP as indicated (Molecular Devices) was added to each assay well. The plates were incubated for 1.5 h at 30 °C. After incubation, IMAP FP phosphodiesterase evaluation assay (Molecular Devices) binding reagent was added to each well and the plates were incubated for an additional 30 min at 30 °C. FP was measured according to the manufacturer's specifications using a Biotek Synergy 4 plate reader.

Experimental Design and Data Analysis. PDE activity was measured, and potency was expressed by an IC_{50} value (50% inhibitory concentration). For enzyme assays, the IC_{50} value was determined by testing a range of 10 concentrations with at least two replicates per concentration. Dose−response curves were analyzed using PrismTM 4 software (GraphPad) to calculate IC_{50} values using a four-parameter logistic equation. All in vitro experiments involved dose−response analysis, which was repeated at least twice to confirm the reproducibility of IC_{50} values.

Cyclooxygenase Assay. The colorimetric COX (ovine) inhibitor screening assay kit (Cayman) was used according to the manufacturer's specification.

Cellular cGMP Elevation Assay. Human kidney embryonic cells (HEK-293 cells, obtained from ATCC) were transfected with the cGMP biosensor (Promega) using Lipofectamine LTX (Invitrogen) to create a HEK-293 cell line, which stably expresses the cGMP biosensor. G418 was used to select positive clones, and clones were screened for luminescence. HEK-293 cells that stably express a cGMP biosensor were seeded at a density of 60,000 cells per well on tissue culture-treated microtiter 96-well plates. Cells were incubated overnight at 37 °C in DMEM media containing 10% FBS. The next day, media were removed and 100 μL of CO_2-independent media with 10% FBS and 5 mM Luciferin (Promega) was added to each well. Cells were incubated at room temperature in the dark for 1 h. Cells were then treated with 50 μM SNP and compound or vehicle control. Luminescence was monitored for 120 min using a Synergy H4 Hybrid plate reader (Bio Tek).

Protein Binding. The protein matrix (human) was spiked with the test compound at 10 μM with a final DMSO concentration of 1%. The dialysate compartment is loaded with phosphate buffered saline (PBS, pH 7.4), and the sample side is loaded with equal volume of the spiked protein matrix. The dialysis plate is then sealed and incubated at 37 °C for 4 h. After the incubation, samples are taken from each compartment, diluted with the phosphate buffer followed by addition of acetonitrile and centrifugation. The supernatants are then used for HPLC−MS/MS analysis. A control sample is prepared from the spiked protein matrix in the same manner as the assay samples (without dialysis). This control sample serves as the basis for the recovery determination. The recovery determination serves as an indicator of reliability of the calculated protein binding value. Low recovery indicates that the test compound is lost during the course of the assay. This is most likely due to non-specific binding or degradation of the test compound.

In Vivo Pharmacokinetic Study. Female, 11−12 week old C57BL/6N mice (weight of 19−21 g, Charles River Laboratory, USA) were used. The animals were housed in a temperature-controlled room (20−24 °C) and maintained in a 12 h light/12 h dark cycle. Food and water were available *ad libitum*. All experimental procedures were approved by IACUC of University of South Alabama, USA (protocol number 933458, approved on August 5, 2016) and conducted in accordance with the regulations of the local animal welfare authorities (the Animal Welfare Act and PHS Policy on Humane Care and Use of Laboratory Animals). **d12** was formulated in ethanol/Maalox (10:90, v/v) at a concentration of 10 mg/mL and administered to six mice by oral gavage at a dose of 150 mg/kg. Blood samples were taken at 1, 2, or 4 h from two mice per time point (as a survival bleeding) and from all six mice at 8 h (terminal bleeding). The blood was collected into K_2EDTA tubes, stored on ice, and subsequently centrifuged at 5000g for 5 min at room temperature, and plasma was separated and kept at below −20 °C until being assayed by liquid chromatography mass spectrometry (LC−MS/MS). **d12** plasma concentrations were quantified using a calibration curve based on calibration standards prepared in drug-free plasma. Results were analyzed using PKSolver 2.0.[33]

Tolerance Study. Female, 8−9 week old athymic nude-Foxn1^{nu} mice (weight of 18−24 g, Harlan Laboratories, USA) were used. The animals were housed in a temperature-controlled room (20−24 °C)

https://doi.org/10.1021/acs.jmedchem.0c01120
J. Med. Chem. 2021, 64, 4462−4477

and maintained in a 12 h light/12 h dark cycle. Food and water were available *ad libitum*. All experimental procedures were approved by IACUC of University of South Alabama, USA (protocol number 933458, approved on August 5, 2016) and conducted in accordance with the regulations of the local animal welfare authorities (the Animal Welfare Act and PHS Policy on Humane Care and Use of Laboratory Animals). Mice were treated with **d12** by oral gavage at doses of 50, 100, or 150 mg/kg twice daily (daily dose of 100, 200, and 300 mg/kg, respectively) or with **d12** vehicle for 28 days. Four mice were included in each group. **d12** was formulated in ethanol/water/Maalox (7:3:90, v/v/v). Mice were monitored daily for signs of toxicity and were weighed daily during the first week of treatment and twice a week for the duration of the study. At the end of the study, all mice were euthanized and necropsy was conducted.

■ ASSOCIATED CONTENT

Supporting Information

The Supporting Information is available free of charge at https://pubs.acs.org/doi/10.1021/acs.jmedchem.0c01120.

Molecular formula strings and PDE5 inhibition data; experimental procedures and analytical data of compounds **a1**−**a25**, **a27**−**a36**, **a38**−**a41**, **a44**−**a50**, **b1**, **c1**−**c5**, **d1**, **d4**−**d7**, **d9**−**d11**, **d13**, **F**, **E1**−**E41**, and **E44**−**E50**; (Figure S1) percent increase in K_m values with rising concentrations of the inhibitor; (Table S1) activity of some selected compounds against COX1 and COX2; (Table S2) PDE5 inhibitory activity of compound **a29** vs its separated enantiomers; (Table S3) fold increase in PDE5 inhibitory potency on extending the carboxylic acids into respective amides with *N*-methylpiperazine; HPLC chromatograms for some selected compounds (PDF)

SMILES (CSV)

■ AUTHOR INFORMATION

Corresponding Authors

Mohammad Abdel-Halim − *Department of Pharmaceutical Chemistry, Faculty of Pharmacy and Biotechnology, German University in Cairo, Cairo 11835, Egypt;* orcid.org/0000-0003-1326-4219; Phone: +201000006222; Email: mohammad.abdel-halim@guc.edu.eg

Ashraf H. Abadi − *Department of Pharmaceutical Chemistry, Faculty of Pharmacy and Biotechnology, German University in Cairo, Cairo 11835, Egypt;* orcid.org/0000-0002-7433-261X; Phone: +202 27589990-8; Email: ashraf.abadi@guc.edu.eg; Fax: +202-27581041

Authors

Sara Sigler − *Departments of Oncologic Sciences and Pharmacology, Mitchell Cancer Institute, University of South Alabama, Mobile, Alabama 36604, United States*

Nora A. S. Racheed − *Department of Pharmaceutical Chemistry, Faculty of Pharmacy and Biotechnology, German University in Cairo, Cairo 11835, Egypt*

Amr Hefnawy − *Department of Pharmaceutical Chemistry, Faculty of Pharmacy and Biotechnology, German University in Cairo, Cairo 11835, Egypt*

Reem K. Fathalla − *Department of Pharmaceutical Chemistry, Faculty of Pharmacy and Biotechnology, German University in Cairo, Cairo 11835, Egypt; Pharmaceutical and Medicinal Chemistry, Saarland University, D-66123 Saarbrücken, Germany*

Mennatallah A. Hammam − *Department of Pharmaceutical Chemistry, Faculty of Pharmacy and Biotechnology, German University in Cairo, Cairo 11835, Egypt*

Ahmed Maher − *Biochemistry Department, Faculty of Pharmacy, October University for Modern Sciences and Arts (MSA), Giza, Egypt*

Yulia Maxuitenko − *Departments of Oncologic Sciences and Pharmacology, Mitchell Cancer Institute, University of South Alabama, Mobile, Alabama 36604, United States*

Adam B. Keeton − *Departments of Oncologic Sciences and Pharmacology, Mitchell Cancer Institute, University of South Alabama, Mobile, Alabama 36604, United States*

Rolf W. Hartmann − *Pharmaceutical and Medicinal Chemistry, Saarland University, D-66123 Saarbrücken, Germany;* orcid.org/0000-0002-5871-5231

Matthias Engel − *Pharmaceutical and Medicinal Chemistry, Saarland University, D-66123 Saarbrücken, Germany;* orcid.org/0000-0001-5065-8634

Gary A. Piazza − *Departments of Oncologic Sciences and Pharmacology, Mitchell Cancer Institute, University of South Alabama, Mobile, Alabama 36604, United States*

Complete contact information is available at: https://pubs.acs.org/10.1021/acs.jmedchem.0c01120

Notes

The authors declare no competing financial interest.

■ ACKNOWLEDGMENTS

Research reported in this publication was supported in part by the National Cancer Institute of the National Institutes of Health under awards R01CA155638, R01CA197147, and R01CA131378. We thank Prof. Greg Gorman, Director of Pharmaceutical Sciences Research Institute, McWhorter School of Pharmacy Samford University (Birmingham, Alabama, USA) for analyzing the plasma level of compound **d12**.

■ ABBREVIATIONS USED

cAMP, cyclic adenosine monophosphate; CC, column chromatography; COX, cyclooxygenase; cGMP, cyclic guanosine monophosphate; DDQ, 2,3-Dichloro-5,6-dicyano-1,4-benzoquinone; EDCI·HCl, *N*-(3-dimethylaminopropyl)-*N*′-ethylcarbodiimide hydrochloride; PK, pharmacokinetics; HEK-293, human kidney embryonic cells; IACUC, Institutional Animal Care and Use Committee

■ REFERENCES

(1) Li, J. J.; Anderson, G. D.; Burton, E. G.; Cogburn, J. N.; Collins, J. T.; Garland, D. J.; Gregory, S. A.; Huang, H.-C.; Isakson, P. C. 1,2-Diarylcyclopentenes as selective cyclooxygenase-2 inhibitors and orally active anti-inflammatory agents. *J. Med. Chem.* **1995**, *38*, 4570−4578.

(2) DeWitt, D. L. COX-2-selective inhibitors: the new super aspirins. *Mol. Pharmacol.* **1999**, *55*, 625−631.

(3) FitzGerald, G. A. Coxibs and cardiovascular disease. *N. Engl. J. Med.* **2004**, *351*, 1709−1711.

(4) Krum, H.; Liew, D.; Aw, J.; Haas, S. Cardiovascular effects of selective cyclooxygenase-2 inhibitors. *Expert Rev. Cardiovasc. Ther.* **2004**, *2*, 265−270.

(5) Zarraga, I. G. E.; Schwarz, E. R. Coxibs and heart disease: what we have learned and what else we need to know. *J. Am. Coll. Cardiol.* **2007**, *49*, 1−14.

(6) Jüni, P.; Nartey, L.; Reichenbach, S.; Sterchi, R.; Dieppe, P. A.; Egger, M. Risk of cardiovascular events and rofecoxib: cumulative meta-analysis. *Lancet* **2004**, *364*, 2021−2029.
(7) Dogné, J.-M.; Supuran, C. T.; Pratico, D. Adverse cardiovascular effects of the coxibs. *J. Med. Chem.* **2005**, *48*, 2251−2257.
(8) Klein, T.; Eltze, M.; Grebe, T.; Hatzelmann, A.; Kömhoff, M. Celecoxib dilates guinea-pig coronaries and rat aortic rings and amplifies NO/cGMP signaling by PDE5 inhibition. *Cardiovasc. Res.* **2007**, *75*, 390−397.
(9) Kimmel, S. E.; Berlin, J. A.; Reilly, M.; Jaskowiak, J.; Kishel, L.; Chittams, J.; Strom, B. L. Patients exposed to rofecoxib and celecoxib have different odds of nonfatal myocardial infarction. *Ann. Intern. Med.* **2005**, *142*, 157−164.
(10) Graham, D. J.; Campen, D.; Hui, R.; Spence, M.; Cheetham, C.; Levy, G.; Shoor, S.; Ray, W. A. Risk of acute myocardial infarction and sudden cardiac death in patients treated with cyclo-oxygenase 2 selective and non-selective non-steroidal anti-inflammatory drugs: nested case-control study. *Lancet* **2005**, *365*, 475−481.
(11) Solomon, D. H.; Avorn, J.; Stürmer, T.; Glynn, R. J.; Mogun, H.; Schneeweiss, S. Cardiovascular outcomes in new users of coxibs and nonsteroidal antiinflammatory drugs: High-risk subgroups and time course of risk. *Arthritis Rheum.* **2006**, *54*, 1378−1389.
(12) Mehats, C.; Andersen, C. B.; Filopanti, M.; Jin, S. L. C.; Conti, M. Cyclic nucleotide phosphodiesterases and their role in endocrine cell signaling. *Trends Endocrinol. Metab.* **2002**, *13*, 29−35.
(13) Conti, M.; Beavo, J. Biochemistry and physiology of cyclic nucleotide phosphodiesterases: essential components in cyclic nucleotide signaling. *Annu. Rev. Biochem.* **2007**, *76*, 481−511.
(14) Francis, S. H.; Turko, I. V.; Corbin, J. D. Cyclic nucleotide phosphodiesterases: relating structure and function. *Prog. Nucleic Acid Res. Mol. Biol.* **2001**, *65*, 1−52.
(15) Rybalkin, S. D.; Rybalkina, I. G.; Shimizu-Albergine, M.; Tang, X. B.; Beavo, J. A. PDE5 is converted to an activated state upon cGMP binding to the GAF A domain. *EMBO J.* **2003**, *22*, 469−478.
(16) Rybalkin, S. D.; Yan, C.; Bornfeldt, K. E.; Beavo, J. A. Cyclic GMP phosphodiesterases and regulation of smooth muscle function. *Circ. Res.* **2003**, *93*, 280−291.
(17) Huang, S. A.; Lie, J. D. Phosphodiesterase-5 (PDE5) inhibitors in the management of erectile dysfunction. *P T* **2013**, *38*, 407−419.
(18) Humbert, M.; Ghofrani, H.-A. The molecular targets of approved treatments for pulmonary arterial hypertension. *Thorax* **2016**, *71*, 73−83.
(19) Wu, D.; Huang, Y.; Chen, Y.; Huang, Y.-Y.; Geng, H.; Zhang, T.; Zhang, C.; Li, Z.; Guo, L.; Chen, J.; Luo, H.-B. Optimization of chromeno[2,3-c]pyrrol-9(2H)-ones as highly potent, selective, and orally bioavailable PDE5 inhibitors: Structure−activity relationship, X-ray crystal structure, and pharmacodynamic effect on pulmonary arterial hypertension. *J. Med. Chem.* **2018**, *61*, 8468−8473.
(20) Wang, Z.; Jiang, X.; Zhang, X.; Tian, G.; Yang, R.; Wu, J.; Zou, X.; Liu, Z.; Yang, X.; Wu, C.; Shi, J.; Li, J.; Suo, J.; Wang, Y.; Zhang, R.; Xu, Z.; Gong, X.; He, Y.; Zhu, W.; Aisa, H. A.; Jiang, H.; Xu, Y.; Shen, J. Pharmacokinetics-driven optimization of 4(3*H*)-pyrimidinones as phosphodiesterase type 5 inhibitors leading to TPN171, a clinical candidate for the treatment of pulmonary arterial hypertension. *J. Med. Chem.* **2019**, *62*, 4979−4990.
(21) Wu, D.; Zhang, T.; Chen, Y.; Huang, Y.; Geng, H.; Yu, Y.; Zhang, C.; Lai, Z.; Wu, Y.; Guo, X.; Chen, J.; Luo, H.-B. Discovery and optimization of chromeno[2,3-c]pyrrol-9(2*H*)-ones as novel selective and orally bioavailable phosphodiesterase 5 inhibitors for the treatment of pulmonary arterial hypertension. *J. Med. Chem.* **2017**, *60*, 6622−6637.
(22) Zheng, H.; Wu, Y.; Sun, B.; Cheng, C.; Qiao, Y.; Jiang, Y.; Zhao, S.; Xie, Z.; Tan, J.; Lou, H. Discovery of furyl/thienyl *β*-carboline derivatives as potent and selective PDE5 inhibitors with excellent vasorelaxant effect. *Eur. J. Med. Chem.* **2018**, *158*, 767−780.
(23) Fiorito, J.; Vendome, J.; Saeed, F.; Staniszewski, A.; Zhang, H.; Yan, S.; Deng, S.-X.; Arancio, O.; Landry, D. W. Identification of a novel 1,2,3,4-tetrahydrobenzo[b][1,6]naphthyridine analogue as a potent phosphodiesterase 5 inhibitor with improved aqueous solubility for the treatment of alzheimer's disease. *J. Med. Chem.* **2017**, *60*, 8858−8875.
(24) Sung, B.-J.; Hwang, K. Y.; Jeon, Y. H.; Lee, J. I.; Heo, Y.-S.; Kim, J. H.; Moon, J.; Yoon, J. M.; Hyun, Y.-L.; Kim, E.; Eum, S. J.; Park, S.-Y.; Lee, J.-O.; Lee, T. G.; Ro, S.; Cho, J. M. Structure of the catalytic domain of human phosphodiesterase 5 with bound drug molecules. *Nature* **2003**, *425*, 98−102.
(25) Turko, I. V.; Ballard, S. A.; Francis, S. H.; Corbin, J. D. Inhibition of cyclic GMP-binding cyclic GMP-specific phosphodiesterase (Type 5) by sildenafil and related compounds. *Mol. Pharmacol.* **1999**, *56*, 124−130.
(26) Blount, M. A.; Beasley, A.; Zoraghi, R.; Sekhar, K. R.; Bessay, E. P.; Francis, S. H.; Corbin, J. D. Binding of tritiated sildenafil, tadalafil, or vardenafil to the phosphodiesterase-5 catalytic site displays potency, specificity, heterogeneity, and cGMP stimulation. *Mol. Pharmacol.* **2004**, *66*, 144−152.
(27) Blount, M. A.; Zoraghi, R.; Ke, H.; Bessay, E. P.; Corbin, J. D.; Francis, S. H. A 46-amino acid segment in phosphodiesterase-5 GAF-B domain provides for high vardenafil potency over sildenafil and tadalafil and is involved in phosphodiesterase-5 dimerization. *Mol. Pharmacol.* **2006**, *70*, 1822−1831.
(28) Wenthur, C. J.; Gentry, P. R.; Mathews, T. P.; Lindsley, C. W. Drugs for allosteric sites on receptors. *Annu. Rev. Pharmacol. Toxicol.* **2014**, *54*, 165−184.
(29) Abdel-Halim, M.; Tinsley, H.; Keeton, A. B.; Weam, M.; Atta, N. H.; Hammam, M. A.; Hefnawy, A.; Hartmann, R. W.; Engel, M.; Piazza, G. A.; Abadi, A. H. Discovery of trisubstituted pyrazolines as a novel scaffold for the development of selective phosphodiesterase 5 inhibitors. *Bioorg. Chem.* **2020**, *104*, 104322.
(30) Huang, Y. R.; Katzenellenbogen, J. A. Regioselective synthesis of 1,3,5-Triaryl-4-alkylpyrazoles: Novel ligands for the estrogen receptor. *Org. Lett.* **2000**, *2*, 2833−2836.
(31) Bischoff, E. Potency, selectivity, and consequences of nonselectivity of PDE inhibition. *Int. J. Impotence Res.* **2004**, *16*, S11−S14.
(32) Abdel-Halim, M.; Keeton, A. B.; Gurpinar, E.; Gary, B. D.; Vogel, S. M.; Engel, M.; Piazza, G. A.; Boeckler, F. M.; Hartmann, R. W.; Abadi, A. H. Trisubstituted and tetrasubstituted pyrazolines as a novel class of cell-growth inhibitors in tumor cells with wild type p53. *Bioorg. Med. Chem.* **2013**, *21*, 7343−7356.
(33) Zhang, Y.; Huo, M.; Zhou, J.; Xie, S. PKSolver: An add-in program for pharmacokinetic and pharmacodynamic data analysis in Microsoft Excel. *Comput. Methods Programs Biomed.* **2010**, *99*, 306−314.

https://doi.org/10.1021/acs.jmedchem.0c01120
J. Med. Chem. 2021, 64, 4462−4477